1521-0103/377/2/293–304$35.00
THE JOURNAL OF PHARMACOLOGY AND EXPERIMENTAL THERAPEUTICS
https://doi.org/10.1124/jpet.120.000238
J Pharmacol Exp Ther 377:293–304, May 2021

SAR340835, a Novel Selective Na^+/Ca^{2+} Exchanger Inhibitor, Improves Cardiac Function and Restores Sympathovagal Balance in Heart Failure[S]

Michel Pelat, Fabrice Barbe, Cyril Daveu, Laetitia Ly-Nguyen, Thomas Lartigue, Suzanne Marque, Georges Tavares, Véronique Ballet, Jean-Michel Guillon, Klaus Steinmeyer, Klaus Wirth, Heinz Gögelein, Petra Arndt, Nils Rackelmann, John Weston, Patrice Bellevergue, Gary McCort, Marc Trellu, Laurence Lucats, Philippe Beauverger, Marie-Pierre Pruniaux-Harnist, Philip Janiak, and Frédérique Chézalviel-Guilbert

Cardiovascular and Metabolism TSU (M.P., F.B., C.D., T.L., S.M., G.T., L.L., Ph.B., M.-P.P.-H., P.J., F.C.-G.) and Integrated Drug Discovery (Pa.B.), Sanofi R&D, Chilly Mazarin, France; Preclinical Safety, Sanofi R&D, Alfortville, France (L.L.-N., V.B., J.-M.G., M.T.); Sanofi R&D, Industriepark Höchst, Frankfurt, Germany (K.S., K.W., H.G., P.A., N.R., J.W.); and Integrated Drug Discovery, Sanofi R&D, Vitry sur Seine, France (G.M.)

Received July 22, 2020; accepted February 8, 2021

ABSTRACT

In failing hearts, Na^+/Ca^{2+} exchanger (NCX) overactivity contributes to Ca^{2+} depletion, leading to contractile dysfunction. Inhibition of NCX is expected to normalize Ca^{2+} mishandling, to limit afterdepolarization-related arrhythmias, and to improve cardiac function in heart failure (HF). SAR340835/SAR296968 is a selective NCX inhibitor for all NCX isoforms across species, including human, with no effect on the native voltage-dependent calcium and sodium currents in vitro. Additionally, it showed in vitro and in vivo antiarrhythmic properties in several models of early and delayed afterdepolarization-related arrhythmias. Its effect on cardiac function was studied under intravenous infusion at 250,750 or 1500 μg/kg per hour in dogs, which were either normal or submitted to chronic ventricular pacing at 240 bpm (HF dogs). HF dogs were infused with the reference inotrope dobutamine (10 μg/kg per minute, i.v.). In normal dogs, NCX inhibitor increased cardiac contractility (dP/dt_{max}) and stroke volume (SV) and tended to reduce heart rate (HR). In HF dogs, NCX inhibitor significantly and dose-dependently increased SV from the first dose (+28.5%, +48.8%, and +62% at 250, 750, and 1500 μg/kg per hour, respectively) while significantly increasing dP/dt_{max} only at 1500 (+33%). Furthermore, NCX inhibitor significantly restored sympathovagal balance and spontaneous baroreflex sensitivity (BRS) from the first dose and reduced HR at the highest dose. In HF dogs, dobutamine significantly increased dP/dt_{max} and SV (+68.8%) but did not change HR, sympathovagal balance, or BRS. Overall, SAR340835, a selective potent NCX inhibitor, displayed a unique therapeutic profile, combining antiarrhythmic properties, capacity to restore systolic function, sympathovagal balance, and BRS in HF dogs. NCX inhibitors may offer new therapeutic options for acute HF treatment.

SIGNIFICANCE STATEMENT

HF is facing growing health and economic burden. Moreover, patients hospitalized for acute heart failure are at high risk of decompensation recurrence, and no current acute decompensated HF therapy definitively improved outcomes. A new potent, Na^+/Ca^{2+} exchanger inhibitor SAR340835 with antiarrhythmic properties improved systolic function of failing hearts without creating hypotension, while reducing heart rate and restoring sympathovagal balance. SAR340835 may offer a unique and attractive pharmacological profile for patients with acute heart failure as compared with current inotrope, such as dobutamine.

Introduction

A variety of treatments are used to improve depressed left ventricular function in heart failure (HF) during periods of acute decompensation. β-Adrenergic agonists, like dobutamine, are currently the gold standard for inotropic agents in acute decompensated HF (AHF); however, their clinical use

This work received no external funding.
No author has an actual or perceived conflict of interest with the contents of this article.
https://doi.org/10.1124/jpet.120.000238.
[S] This article has supplemental material available at jpet.aspetjournals.org.

ABBREVIATIONS: AHF, acute decompensated HF; AVB, atrioventricular block; BRS, baroreflex sensitivity; CO, cardiac output; DAD, delayed afterdepolarization; DBP, diastolic blood pressure; dP/dt_{max}, maximal rate of rise of left ventricular pressure; dP/dt_{min}, minimal rate of rise of (usually) left ventricular pressure; DT, deceleration time; E/A, the ratio of peak velocity blood flow from left ventricular relaxation in early diastole (the E wave) to peak velocity flow in late diastole caused by atrial contraction (the A wave); EAD, early afterdepolarization; E-C, excitation-contraction; HF, heart failure; HFpEF, HF with preserved ejection fraction; HR, heart rate; LAV, left atria vulnerability; LF, low frequency; LV, left ventricle; LVEDV, left ventricular end-diastolic volume; LVEF, left ventricular ejection fraction; MAD, median absolute deviation; MVO2, Myocardial oxygen consumption; NCX, Na^+/Ca^{2+} exchanger; nu, normalized unit; PR, progesterone; SBP, systolic blood pressure; SV, stroke volume; TdP, Torsades de Pointe.

is limited by major drawbacks. Firstly, β-adrenergic receptor desensitization requires continuous augmentation of the dose to maintain inotropic efficacy. Secondly, stimulation of adrenergic receptors induces tachycardia and increases myocardial oxygen consumption out of proportion to their positive inotropic action, potentially reducing cardiac efficiency at midterm. Finally, they exert deleterious effects on membrane electrical stability, favoring the occurrence of arrhythmias and cardiovascular death (Van Bilsen et al., 2017).

It is well known that hemodynamic alterations accompanying HF are associated with abnormal regulation of intracellular Ca^{2+}, leading to electrophysiological and excitation-contraction (E-C) alterations at the cellular level. Reduction of the amplitude of intracellular Ca^{2+} transient and of its rate of decay have been reported in isolated myocytes from failing human and dog hearts (O'Rourke et al., 1999; Menick et al., 2007; (Bögeholz et al., 2017)). The cardiac plasma membrane Na^+/Ca^{2+} exchanger (NCX) is the main Ca^{2+} extrusion mechanism of the cardiac myocyte and is crucial for maintaining Ca^{2+} homeostasis. NCX is a key player of cardiac E-C coupling that regulates cytosolic Ca^{2+} and Na^+ concentration, repolarization process, and contractility (Wei et al., 2007; Ottolia et al., 2013). Moreover, NCX expression and activity are consistently upregulated in both patients with HF (Sipido et al., 2002; Pott et al., 2011) and animal models of HF (O'Rourke et al., 1999; Goldhaber and Philipson, 2013; (Bögeholz et al., 2017)). This overactivity, which is associated with a reduced efficacy of sarcoplasmic reticulum Ca^{2+}-ATPase to pump cytosolic Ca^{2+} back into the sarcoplasmic reticulum during diastole, favors excessive Ca^{2+} extrusion from the cytosol, which leads to a reduction in sarcoplasmic reticulum Ca^{2+} content and thereby contributes to cardiac contractility impairment.

In addition, increased NCX current favors generation of early afterdepolarization (EAD)-related arrhythmias and delayed afterdepolarization (DAD)-related arrhythmias. Enhanced expression of NCX is recognized as one of the molecular mechanisms that increases the risk of arrhythmias during the development of HF with reduced ejection fraction (Hobai et al., 2004; Peana and Domeier, 2017). Therefore, NCX blockers have been proposed as positive inotropes and antiarrhythmic agents in the treatment of HF. The therapeutic objective in patients with HF is therefore to limit NCX overactivity to maintain adequate sarcoplasmic reticulum Ca^{2+} refilling, to improve cardiac dysfunction, and additionally to reduce the risk of arrhythmias through restoration of proper calcium-induced calcium release. Indeed, partial inhibition of NCX increases intracellular Ca^{2+} available for sarcoplasmic reticulum Ca^{2+}-ATPase and improves systolic and diastolic function in both normal and failing canine cardiomyocytes (O'Rourke et al., 1999; Hobai et al., 2004) and prevents the occurrence of EAD- and DAD-related arrhythmias, which are commonly observed in patients with HF (Kohajda et al., 2016). Only one NCX inhibitor, caldaret, has been clinically developed that aims at normalizing disturbed calcium handling in patients with either myocardial infarction or HF. Although caldaret was shown to be safe in patients, the compound was stopped due to its limited efficacy on myocardial infarction size or LV dysfunction ((Bär et al., 2006)). However, the limited literature about caldaret did not allow a conclusion as to whether its potency and specificity to inhibit NCX were appropriate to increase cardiac function in these patients. Recently, highly specific and potent NCX inhibitors were reported (Primessnig et al., 2019; Otsomaa et al., 2020). They clearly improved cardiac function in both the normal and HF condition in rat and rabbit and showed antiarrhythmic properties (Kohajda et al., 2016).

SAR340835 is a water-soluble prodrug of SAR296968, a potent, selective, short-acting NCX inhibitor (Czechtizky et al., 2013). At 30 minutes after intravenous injection, SAR340835 is totally transformed into SAR296968, its active moiety, which is responsible for its NCX inhibitory activity.

The purpose of this study was to evaluate the antiarrhythmic, hemodynamic, and cardiac effects of SAR340835 in conscious normal dogs and in dogs with rapid right ventricular pacing–induced heart failure. The antiarrhythmic properties were investigated in experimental models using mammalian species with electrophysiological properties close to human (guinea pig, rabbit, pig). To examine E-C coupling in more detail, ex vivo contractility studies in response to SAR296968 were also performed on normal and failing canine cardiomyocytes. SAR340835 profiling was performed in comparison with dobutamine, which was used as a calibrator in the rapid right ventricular pacing–induced HF dogs.

Materials and Methods

The purpose of this study was to evaluate the therapeutic potential for AHF of SAR340835, a new potent NCX inhibitor, by successively profiling its in vitro potency and specificity, evaluating its antiarrhythmic properties, and determining the cardiodynamic profile in normal and HF dogs. As we were hypothesizing that NCX inhibition could be beneficial in patients with acute heart failure, the canine heart failure studies were performed versus dobutamine, a well known therapeutic reference for AHF. Electrophysiological investigations were performed in mammalian species with electrophysiological features close to humans, i.e., showing a marked plateau of action potential (guinea pig, rabbit, dog, pig) and in which NCX is known to behave as in human heart (Bers et al., 2006).

The successive steps of our methodological approach to fully characterize SAR340835, the prodrug of SAR296968, are illustrated by Fig. 1. A brief summary of methods is provided here. The full experimental conditions of those experiments are detailed in Supplemental Material.

Ethical Approvals

All the procedures described in the present study were performed in agreement with the European regulation (2010/63/UE) and under the approval and control of SANOFI's ethics committee. All procedures were performed in Association for Assessment and Accreditation of Laboratory Animal Care International-accredited facilities in full compliance with the standards for the care and use of laboratory animals and in accordance either with the French Ministry for Research or with the German animal protection law.

In Vitro Characterization of SAR296968, the Active Principle of SAR340835

An extended method for these in vitro studies is available in Supplemental Material. Briefly, in vitro potency on the NCX isoforms was assessed by a cell-based calcium mobilization assay on CHO cell lines expressing either NCX1, NCX2, or NCX3 with a fluorescent imaging plate reader and using the Ca^{2+}-sensitive dye Fluo4-AM for measurement of the intracellular Ca^{2+} concentration. The specificity of action toward NCX was investigated in guinea pig cardiomyocytes by performing patch-clamp studies to evaluate the activity of SAR296968 on the endogenous NCX, calcium, and sodium currents.

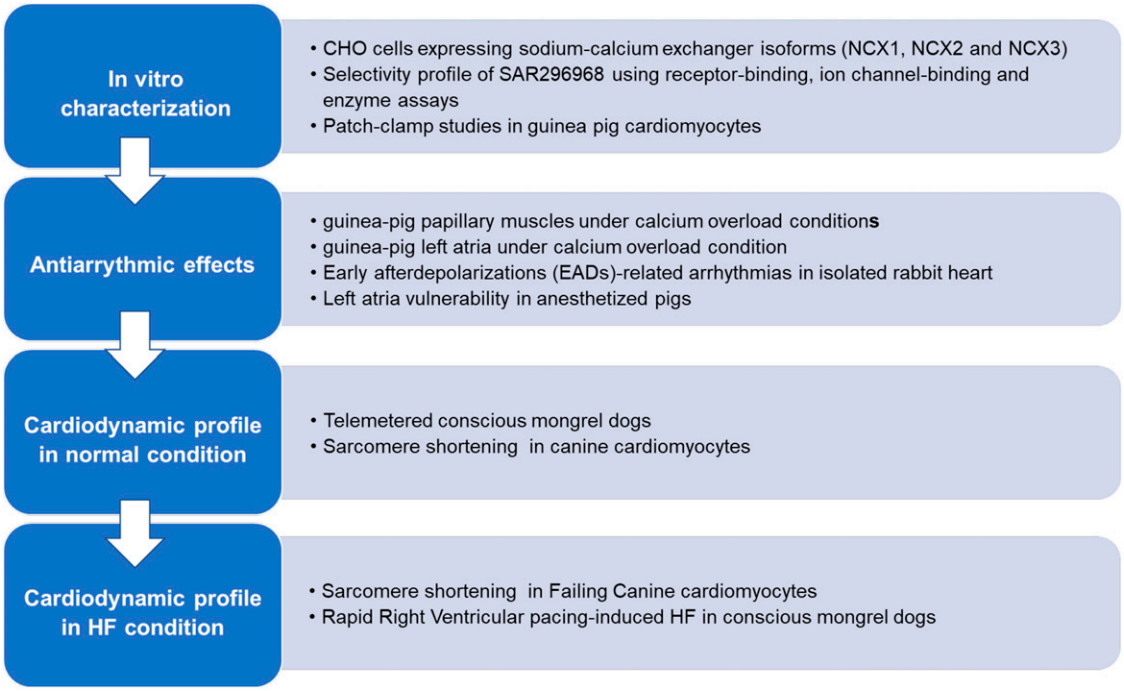

Fig. 1. Brief summary of our methodological approach to fully characterize SAR340835, the prodrug of SAR296968.

Moreover, an extended profiling of SAR296968 was carried out using receptor binding, ion channel binding, and enzyme assays (Supplemental Table 6).

Effects of SAR296968 on Atrial and Ventricular Arrhythmias

Confirmatory Studies. The antiarrhythmic properties of the NCX inhibitor were assessed in a battery of in vitro and in vivo models using the active principle SAR296968. NCX inhibition was extensively described in literature to reduce the occurrence of early and delayed afterdepolarization. We performed confirmatory studies with our compound in guinea pig papillary muscles and left atria under calcium overload condition to determine its ability to reduce DAD-related arrhythmias. Furthermore, the efficacy of SAR296968 against EADs was tested in isolated rabbit heart perfused according to the Langendorff method. The extended methods for those experiments are described in Supplemental Material.

Left Atria Vulnerability in Anesthetized Pigs. The antiarrhythmic property of SAR296968 was further investigated by measuring the left atria vulnerability (LAV) in pentobarbital-anesthetized pigs. The purpose of this investigation was to determine the effect of NCX inhibition on atrial refractoriness and electrically induced atrial arrhythmias. Pigs were premedicated with 2 ml Rompun 2%, i.m. (xylazine HCl, 23.3 mg/ml) and 1 ml of Zoletil 100 (100 mg/ml; 50 mg/ml tiletamine and 50 mg/ml zolazepam) and anesthetized with an intravenous bolus of 3 ml Narcoren (pentobarbital, 160 mg/ml), followed by a continuous intravenous infusion of 12–17 mg/kg per hour pentobarbital. Pigs were ventilated with room air and oxygen by a respirator. Blood gas analysis (partial pressure of oxygen or pO_2; partial pressure of carbon dioxide or pCO_2) was performed at regular time intervals to control the oxygen supply via the respirator to maintain $pO_2 > 100$ mm Hg and $pCO_2 < 35$–40 mm Hg. A left thoracotomy was performed at the fifth intercostal space, the lung was retracted, the pericardium was incised, and the heart was suspended in a pericardial cradle. The atrial effective refractory period, determined by the S1-S2 method, and cardiac contractility (dP/dt_{max}) were monitored at baseline and under treatment with SAR296968 (1.5 mg/kg over 20 minutes) dissolved in a mixture of DMSO (1 ml) and PEG400 (9 ml). LAV was determined as described previously (Wirth et al., 2007). Briefly, the S1-S2 stimulation procedure induced short self-terminating episodes of atrial tachycardia (fibrillation or flutter). The number of atrial repetitive action potentials after the premature beat S2 had to exceed 4 for a full score (1). Three or four repetitive action potentials were counted as a half score (0.5). The procedure was applied while increasing the coupling S1-S2 interval by 5 milliseconds and was repeated at three basic cycle lengths (150, 200, and 250 bpm). A total of 45 S1-S2 stimulation procedures were repeated before and after infusion of SAR296968 in eight pigs. The same procedure was performed on a separate control group of seven pigs according to the same protocol with infusion of the vehicle.

Effect of SAR340835 on Cardiac Hemodynamics in Normal and HF Dogs

Animal and Surgical Procedure. In total, 12 adult mongrel dogs (body weight 27–31 kg) were implanted with telemetry devices (L21-F2; Datasciences International). Six of them were additionally equipped with a pacemaker (Adapta model; Medtronic, MI) with bipolar epicardial Pacing Lead (CapSure Epi; Medtronic) for induction of heart failure by tachypacing: 240 beats per minute for 4 weeks.

For drug infusion, dogs were implanted under anesthesia with a vascular access port.

Rapid Right Ventricular Pacing–Induced HF. Heart failure was induced by chronic rapid right ventricle pacing at 240 beats per minute for 4 weeks with the programmable pacemaker. Baseline echocardiogram and hemodynamic recordings were performed before and at the end of the 4-week pacing period to assess the development of heart failure.

Study Design in Normal and Pacing-Induced HF Dogs. The same study design was applied to normal and HF dogs. All the experiments were performed in conscious animals 4 weeks after the induction of HF by rapid pacing. Dogs were trained daily to remain quiet during the hemodynamic and echocardiography procedures before and after surgery. Before each echocardiography and telemetry monitoring session, pacing was turned off and maintained off during the whole recording period.

Each animal was subjected to four treatment sessions over the following 2 weeks with vehicle or SAR340835 infused at 250, 750, or 1500 μg/kg per hour. Pacing-induced heart failure dogs received dobutamine infused at 10 μg/kg per minute during an additional session for comparison purposes. SAR340835 was intravenously administered with a loading dose over 2 minutes (0.29, 0.86, or 1.73 mg/kg for 250, 750, and 1500 μg/kg per hour, respectively), followed by an intravenous infusion maintained for 3 hours in HF dogs and 6 hours in normal dogs (250, 750, or 1500 μg/kg per hour, respectively). For simplification, doses are designated by the maintenance infusion rate in the tables and figures. A minimum washout period of 2 days in accordance with the short half-life of compounds was allowed between two sessions.

During each session, after a 15-minute stabilization period, telemetry signals were continuously recorded throughout the treatment infusion. Echocardiography was performed before starting the treatment infusion and over the last minutes of the 3- or 6-hour treatment infusion.

Echocardiography Measurements. Cardiac function was assessed by echocardiography using a Philips CX 50 (Philips, Amsterdam, The Netherlands) with a 5-MHz phased-array transducer. Additional methodological details are provided online in Supplemental Methods.

Telemetry Recordings and Analysis. Telemetry signals (LVP, ECG, aortic blood pressure) were continuously recorded throughout the experiment starting 15 minutes before and until the end of vehicle or treatment infusion at a sampling rate of 500 Hz. Measurements were averaged over at least 20-second periods using HEM software (Notocord System, Croissy, France). Several derived parameters were calculated: diastolic (DBP) and systolic (SBP) aortic blood pressure, left ventricular end-diastolic pressure (LVEDP), dP/dt_{max}, and dP/dt_{min}.

Myocardial oxygen consumption (MVO2 in milliliters of O_2/min per 100 g) was calculated using the following equation developed by Rooke and Feigl (1982):

$$\text{MVO2} = 0.000408*(\text{SBP}*\text{HR}) + 0.000325*([(0.8*\text{SBP} + 0.2*\text{DBP})*\text{HR}*\text{SV}]/\text{BW}) + 1.43.$$

Evaluation of Autonomic Tone and Baroreflex. The effects of SAR340835 on the autonomic nervous system (ANS) were explored. Spectral analysis of heart rate variability was performed for the evaluation of autonomic tone in all telemetered dogs before and at the end of the 3 hours of dosing. This spectral analysis using a fast-Fourier transform algorithm on sequences of 512 points (5 minutes) was performed with the HEM CsA10 software (Notocord Systems, Croissy, France).

Specific frequency bands of heart rate variability permitted the simultaneous assessment of sympathetic [Low Frequency] and parasympathetic [High Frequency] modulation, with the Low Frequency/High Frequency ratio illustrating the sympathovagal balance. Spectral powers were determined as the area under the curve calculated for the very low frequency (0.04–0.05 Hz), low frequency (0.05–0.15 Hz), and high frequency (0.15–0.5 Hz) bands. The results are expressed in normalized units (nu) for spectral indices calculated as follows:

$$\text{Low Frequency (nu, \%)} = (\text{Low Frequency}/(\text{Low Frequency} + \text{High Frequency}))*100;$$

$$\text{High Frequency (nu, \%)} = (\text{High Frequency}/(\text{Low Frequency} + \text{High Frequency}))*100.$$

To investigate the ability of heart rate changes to counteract arterial blood pressure variations, spontaneous baroreflex efficiency was evaluated using the sequence method (Verwaerde et al., 1999; Gronda et al., 2014). Additional methodological details are provided online in Supplemental Methods.

ECG Analysis. The ECG signals of all animals were examined for any test article–related abnormality in wave form morphology. The progesterone (PR) interval was evaluated on each dosing day, at least at each selected time point, over a 60-second period. Examination of second-degree AVB was performed on the totality of the 24-hour recording of ECG.

Dog Cardiomyocyte Studies

Detailed methods of dog cardiomyocyte studies are provided in the Supplemental Material.

Statistical Analysis

Detailed statistical analysis is described in Supplemental Methods.

Results

In Vitro Profile of SAR296968

NCX Inhibition Potency of SAR296968. In CHO cell lines expressing sodium-calcium exchanger isoforms, SAR296968 potently inhibited the human NCX1, with an IC_{50} of 74 nM (Fig. 2). Inhibition of human NCX2 and NCX3 occurred within similar ranges. Testing of SAR296968 on NCX1 orthologs from dog, guinea pig, pig, rabbit, and rat also showed the same range of inhibitory potency (Fig. 2).

In voltage-clamp studies in guinea pig cardiomyocytes, SAR296968 inhibited both the forward and reverse mode of the NCX current in a concentration-dependent manner with similarly high potency. For the forward mode (recorded at the potential of −90 mV), an IC_{50} value with 95% confidence interval of 34.9 nM (29.0; 42.0) was yielded. For the reverse mode (recorded at the potential of +45 mV), the curve fit yielded an IC_{50} value with 95% confidence interval of 38.9 nM (30.6; 49.5) (Fig. 2).

Selectivity of SAR296968. At a concentration more than 100-fold higher than the IC_{50} on NCX, SAR296968 had no or only a minimal effect on the native voltage-dependent calcium and sodium currents in guinea pig cardiomyocytes (Fig. 2).

The target profiling showed that SAR296968 (10 μM) had only a weak antagonist effect on 5-Hydroxytryptamine receptor 2B (IC_{50} = 4 μM) and benzodiazepine peripheral receptor (IC_{50} = 6 μM) and weak inhibition of norepinephrine uptake (IC_{50} > 30 μM) and dopamine uptake (IC_{50} = 17 μM). No functional effects on PR (IC_{50} of 1.4 μM in binding assay) were reported. There are no functional assays available for androgen receptor (IC_{50} of 0.18 μM in binding assay), but potential effects should be limited because of the short duration of the anticipated treatment in patients (48 hours). The binding profile of SAR340835 is comparable to the one of SAR296968.

Antiarrhythmic Properties of SAR296968

SAR296968 was effective to reduce DAD-related arrhythmias in both models at doses that increased cardiac contractility. Thus, in guinea pig papillary muscles, a positive inotropic effect was observed at all tested SAR296968 concentrations (dP/dt_{max} changes versus vehicle group: +29% and +47% at 1 and 3 μM SAR296968, respectively; Supplemental Table 2). In parallel, the number of arrhythmic contractions triggered by high calcium/low potassium concentrations was strongly reduced from 20.5 ± 0.0 (median ± MAD, n = 12) in the vehicle control group to 0.0 ± 0.0 at 1 μM (median ± MAD,

A

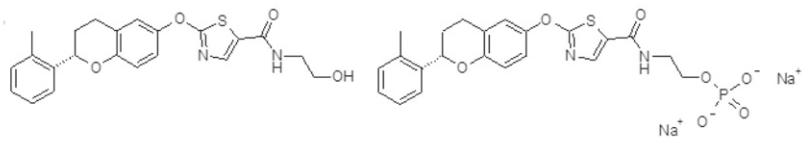

B

Species NCX	IC50 [nM]	Confidence Intervals [nM]	Number of experiments
Human NCX1	74	[54; 102]	n=11
Human NCX2	23	[17; 31]	n=4
Human NCX3	129	[84; 199]	n=5
Dog NCX1	21	[16; 29]	n=4
Guinea-pig NCX1	156	[129; 188]	n=7
Pig NCX1	68	[42; 110]	n=3
Rabbit NCX1	142	[120; 166]	n=7
Rat NCX1	211	[183; 242]	n=7

C Dose/Response relationship for SAR296968 on NCX1 current

	IC50 [nM]	Confidence Intervals [nM]
NCX1 Forward (-90 mV)	34.9	[29.0; 42.0]
NCX1 Reverse (+45 mV)	38.9	[30.6; 49.5]

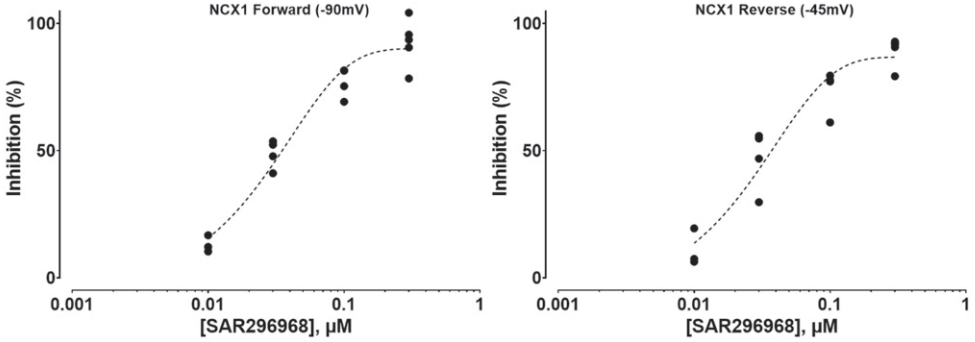

D Effect of SAR296968 at 10 µM on ICa and INa currents (Current change values, Mean %)

Current change [%]	SAR296968 10µM	Nifedipine 10µM	Tetrodotoxin 10µM	N
ICa	-1.75 ± 5.21	-78.70 ± 3.824		7
INa	6.76 ± 6.00		-86.94 ± 1.70	4

Fig. 2. SAR296968 in vitro characterization. (A) Chemical structure of SAR296968 (active principle, left) and SAR340835 (prodrug, right). (B) Inhibition potency of SAR296968 on NCX isoforms in CHO cells. Effect of SAR296968 on the native NCX1 current (C) and on calcium current (ICa) and sodium current (INa) (D).

$n = 8$, $P = 0.0054$ vs. vehicle) and to 0.0 ± 0.0 at 3 µM (median ± MAD, $n = 8$, $P = 0.0054$ vs. vehicle; Table 1). Similarly, guinea pig left atria treated with 3 µM SAR296968 responded with a 1.28-fold increase in dP/dt_{max} from baseline versus a 0.84-fold change recorded under vehicle treatment, and a 90% reduction of the spontaneous arrhythmic contractions induced by isoprenaline [1.5 ± 1.5 spontaneous arrhythmic contractions after 3 µM SAR296968 (median ± MAD, $n = 10$) vs. 15.5 ± 4.5 in the separate vehicle control group (median ± MAD, $n = 10$) (Table 1)].

In isolated rabbit hearts, sotalol-induced TdP occurred in the six hearts tested when the pacing rate and the K^+ concentration were decreased. Their occurrence was limited by SAR296968 pretreatment at 0.3 µM (TdP in two of six hearts) or 1 µM (TdP in one of six hearts) (Fig. 3). In parallel, SAR296968 reduced in a concentration-dependent manner the sotalol prolonging effect on QT interval duration by −46 and −95 milliseconds for 80 bpm at 0.3 and 1 µM, respectively. Moreover, SAR296968 blunted the sotalol-induced increase in dispersion of ventricular repolarization, although not significantly, except for the 0.3 µM dose at 40 bpm (T wave peak to T wave end) interval duration (Tp-Te) reduced by −27 milliseconds at 0.3 µM and −20 milliseconds at 1 µM SAR296968). The QRS interval duration was not affected by SAR296968 administration (Supplemental Table 3). The same level of antiarrhythmic efficacy was shown when TdP were induced by veratridine application (Fig. 3), which was associated with reduction of the veratridine-induced prolongation of the QT interval duration, without affecting the dispersion of ventricular repolarization or the QRS interval (Supplemental Table 3a).

TABLE 1

Antiarrhythmic effects of SAR296968 in animal models of arrhythmias related to early or late afterdepolarizations

In guinea pig papillary muscle and left atria, SAR296968 exhibited antiarrhythmic properties at 1 and 3 μM. In a pig model of electrically induced episodes of atrial fibrillation, SAR296968 (1.5 mg/kg, i.v.) exhibited strong antiarrhythmic effects.

		n	Median	±	MAD
Number of arrhythmic contractions in guinea pig papillary muscle	Vehicle	12	20.5	±	0.0
	SAR296968 1 μM	8	No arrhythmic contraction		
	SAR296968 3 μM	8	No arrhythmic contraction		
Number of arrhythmic contractions in guinea pig left atria	Vehicle	10	15.5	±	4.5
	SAR296968 3 μM	10	1.5	±	1.5
		n	Mean	±	S.E.M.
Number of inducible atrial fibrillation episodes in anesthetized pig	Baseline	8	25.5	±	1.75
	SAR296968 (1.5 mg/kg, i.v.)	8	6.56*	±	1.99

*$P < 0.05$ vs. baseline.

In anesthetized pigs, SAR296968 1.5 mg/kg significantly increased left ventricular contractility by 49%, raising the dP/dt_{max} from 1423 ± 144 mm Hg/s at baseline to 2115 ± 189 mm Hg/s after infusion completion. No changes in the left or right atrial effective refractory period were recorded after SAR296968 treatment regardless of the basic cycle length (Supplemental Table 3b). However, the incidence of atrial arrhythmias (LAV) was significantly reduced after SAR296968 administration by 74% (6.56 ± 1.99 events after SAR296968 administration vs. 25.50 ± 1.75 events at baseline, $n = 8$, $P < 0.001$) (Table 1). No significant changes in either atrial effective refractory period (AERP) (Supplemental Table 3b) or LAV (23.29 ± 6.02 events after vehicle administration vs. 27.00 ± 3.66 events at baseline, $n = 7$, non significant) were observed in the vehicle-treated group.

Effects of SAR340835 in Normal Conscious Dogs

Infusion of SAR340835 had no effect on arterial pressure but dose-dependently decreased heart rate with a significant effect only at the highest dose (−23.4%, $P = 0.0164$) (Table 2). Compared with vehicle, SAR340835 significantly increased dP/dt_{max} at 250, 750, and 1500 by +24.4% ($P = 0.0479$), +38.7% ($P = 0.0054$), and +65.6% ($P = 0.0003$), respectively (Fig. 4; Table 2). In parallel, stroke volume (SV) was significantly increased to an almost similar magnitude regardless of the dose [+16.5% ($P = 0.0144$), +21.7% ($P = 0.0026$), and +14.1% ($P = 0.0327$) at 250, 750, and 1500 μg/kg per hour, respectively (Table 2)]. SAR340835 increased dP/dt_{max} and left ventricular end-diastolic volume (LVEDV) in a dose-dependent manner, only reaching statistical significance at 750 and 1500 μg/kg per hour [+27% and +36.3% increase compared with vehicle, respectively (Table 2)]. SAR340835 had no effect on calculated oxygen consumption (MVO2) (Table 2).

SAR340835 significantly increased dP/dt_{min} at 750 and 1500 μg/kg per hour by 7.2% ($P = 0.0238$) and 9.6% ($P = 0.0066$), respectively (Table 2). However, SAR340835 did not induce any changes in the other echocardiographic parameters of diastolic function (Table 2).

SAR340835 prolonged PR interval duration in a dose-dependent manner, reaching significance at 1500 μg/kg per hour [+28.5% ($P = 0.0116$)] (Fig. 4; Table 2). Second-degree AVBs (isolated P-waves) were attributed to SAR340835 in two of four normal mongrel dogs and occurred during infusions of both 750 and 1500 μg/kg per hour. One dog did not exhibit any second-degree AVB whatever the dose, and one dog already had preexisting second-degree AVB, either in the vehicle-treated session or before treatment at each session. For the two other dogs, second-degree AVB occurred generally early after starting SAR340835 infusion (6–35 minutes for three experiments, and 3 hours in one animal) and with a frequency ranging from two to three isolated P-waves per 20 seconds to 6–12 isolated P-waves per 20 seconds.

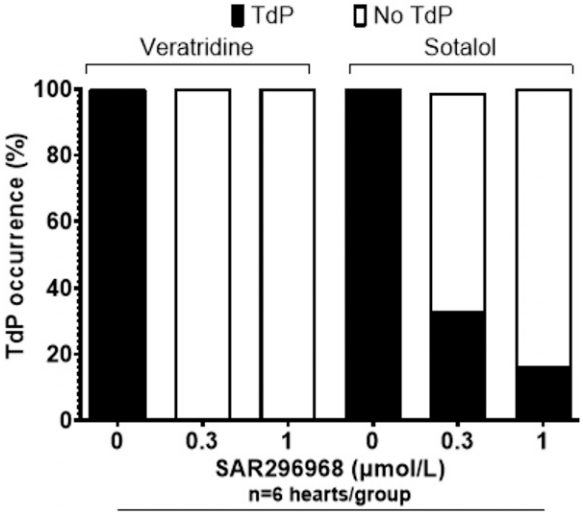

Fig. 3. Effect of SAR296968 on EAD-related arrhythmias in the isolated rabbit heart model SAR296968 in isolated rabbit heart: SAR296968 treatment at 0.3 or 1 μM decreased the sotalol-induced TdP without any proarrhythmic activity by suppression of EAD induced by veratridine.

Effects of SAR340835 in Pacing-Induced HF Dogs

HF Dog Model Characteristics. After 4 weeks of rapid right ventricular pacing at 240 bpm, HF dogs' phenotype recapitulated the clinical signs of dilated cardiomyopathy and heart failure in humans (Table 3). The dogs exhibited a major increase in LVEDV from 75 ± 6 ml at baseline (i.e., before starting the pacing) to 119 ± 6 ml ($P = 0.0010$), a depressed contractility illustrated by a marked decrease in dP/dt_{max} and dP/dt_{max}/LVEDV (Table 3), and a significant and profound decrease in LVEF from 55% ± 3% to 28% ± 1% ($P = 0.0001$). This decrease in cardiac contractility is also reflected by a significantly reduced SV from 64 ± 2 ml to 31 ± 3 ml ($P = 0.0012$). HF dogs also displayed a severe diastolic dysfunction illustrated by a restrictive pattern (E/A > 1) and a reduced deceleration time (DT) from 83.6 ± 7.1 to 54.3 ± 4.4 milliseconds ($P = 0.0076$). In addition, ANS modifications typical of human HF were also observed.

TABLE 2

Cardiac and hemodynamic effects of SAR340835 in normal dogs

Autonomic nervous system was evaluated by heart rate variability analysis. All data are expressed as means ± SEM and median ± MAD for Low Frequency/High Frequency ratio ($P < 0.05$ vs. vehicle group; n = 3–5 dogs according to the group or parameter considered).

			Normal Dogs		
		Vehicle infusion	SAR340835 Infusion		
	n		250 μg/kg per hour	750 μg/kg per hour	1500 μg/kg per hour
Hemodynamics					
dP/dt_{max} (mm Hg/s)	3 to 4	3091 ± 311	3856 ± 450*	4340 ± 264**	5143 ± 514***
dP/dt_{min} (mm Hg/s)	3	−2648 ± 153	−2674 ± 106	−2840 ± 178*	−2902 ± 124**
LVEDP (mm Hg)	3	10 ± 0.7	9.5 ± 0.32	9.7 ± 0.5	9 ± 0.4
SBP (mm Hg)	4	119 ± 4.0	113 ± 6	131 ± 3	125 ± 4
DBP (mm Hg)	4	83 ± 2.8	75 ± 5	93 ± 1	84 ± 5
PR interval (ms)	4	100 ± 3	106 ± 5	124 ± 9	130 ± 13*
dP/dt_{max}/LVEDV (mm Hg/s per milliliter)	3 to 4	40.8 ± 4.1	47.3 ± 5.6	56.7 ± 5.2**	57 ± 4.7**
MVO2 (ml O_2/min per 100 gram)	4 to 5	13.85 ± 1.16	12.72 ± 0.84	13.97 ± 2.09	12.5 ± 0.86
Echocardiography					
SV (ml)	4 to 5	63 ± 2	73 ± 3*	77 ± 2**	72 ± 3*
HR (bpm)	4 to 5	93 ± 8	83 ± 5	76 ± 12	74 ± 6*
CO (l/min)	4 to 5	5.8 ± 0.6	6 ± 0.4	6 ± 1	5.3 ± 0.8
LVEF (%)	4 to 5	58 ± 3	62 ± 2	66 ± 3	64 ± 1
LVEDV (ml)	4 to 5	73 ± 2	77 ± 4	78 ± 4	82 ± 9
E (cm/s)	4 to 5	0.85 ± 0.02	0.825 ± 0.025	0.92 ± 0.04	0.86 ± 0.04
DT (ms)	4 to 5	80.1 ± 8.1	83.7 ± 10.5	93.8 ± 15.2	78.7 ± 9.0
A (cm/s)	4 to 5	0.58 ± 0.07	0.58 ± 0.06	0.59 ± 0.01	0.70 ± 0.075*
E/A	4 to 5	1.54 ± 0.16	1.58 ± 0.18	1.60 ± 0.17	1.28 ± 0.16
Heart rate variability					
Low Frequency (nu)	3 to 4	22 ± 3	14 ± 1	16 ± 4	14 ± 5
High Frequency (nu)	3 to 4	75 ± 3	83 ± 2	81 ± 5	83 ± 5
Low Frequency/High Frequency	3 to 4	0.32 ± 0.06	0.17 ± 0.03	0.15 ± 0.04	0.16 ± 0.10
BRS (mm Hg/s)	3 to 4	50 ± 2	53 ± 2	63 ± 10	55 ± 6

High Frequency, parasympathetic modulation; Low Frequency, sympathetic modulation; Low Frequency /High Frequency, sympathovagal balance; nu, normalized unit.
*$P < 0.05$, **$P < 0.01$, and ***$P < 0.001$ SAR340835 vs. vehicle.

Additional pathologic features of dogs included tachycardia, loss of the normally observed respiratory sinus arrhythmia, ANS imbalance as shown by an Low Frequency/High Frequency ratio that was increased from 0.22 ± 0.12 in normal dogs to 2.29 ± 0.45 in HF dogs ($P < 0.0001$) and impaired baroreflex sensitivity (49 ± 3 in normal dogs vs. 24 ± 3 in HF dogs, $P < 0.0001$).

Effects of SAR340835 and Dobutamine on Hemodynamics of Conscious HF Dogs. The effects of SAR340835 and dobutamine on hemodynamic parameters in dogs with HF are shown in Table 4. Neither SAR340835 nor dobutamine altered systolic or diastolic arterial pressure compared with vehicle regardless of the dose tested (Table 4). SAR340835 infusion over 3 hours tended to decrease heart rate (HR) from 250 μg/kg per hour (Fig. 4; Table 4), whereas dobutamine did not affect HR.

Effects of SAR340835 and Dobutamine on Left Ventricular Systolic Function of Conscious HF Dogs. Infusion of SAR340835 overall increased dP/dt_{max} in a dose-dependent manner, but this effect reached statistical significance only at the highest dose tested. dP/dt_{max} at the end of 1500 μg/kg per hour infusion reached 1699 ± 208 mm Hg/s in comparison with 1276 ± 79 mm Hg/s at the completion of vehicle infusion ($P = 0.0125$), (Fig. 5; Table 4). dP/dt_{max}/LVEDV increased in a dose-dependent manner, but it reached statistical significance only at the highest dose tested (+26.4%, $P = 0.0057$; Table 4).

Infusion of dobutamine significantly increased LV dP/dt_{max} at 10 μg/kg per minute (59.6% vs. vehicle, $P = 0.0177$) (Table 4). SAR340835 dose-dependently and significantly increased SV at 250, 750, and 1500 μg/kg per hour by 28.5% ($P = 0.0393$), 48.8% ($P = 0.0022$), and 62.2% ($P = 0.0002$), respectively (Fig. 5; Table 4). As heart rate decreased with SAR340835 infusion, the increase in stroke volume translated into a moderate cardiac output (CO) increase (+21.7%, +5.5%, and +26.1% at 250, 750, and 1500 μg/kg per hour, respectively) that did not reach statistical significance (Fig. 5; Table 4). SAR340835 dose-dependently increased LVEF (+33.9%, $P = 0.0182$, and +41%, $P = 0.0034$) at 750 and 1500 μg/kg per hour, respectively. SAR340835 did not change calculated oxygen consumption (MVO2) (Table 4).

After 3 hours of infusion, dobutamine at 10 μg/kg per minute significantly increased SV by 68.8% ($P = 0.0030$) and CO by 75.1% ($P = 0.0031$) and increased LVEF by 47.3% without reaching significance ($P = 0.0679$). Dobutamine significantly increased calculated MVO2 by 28.14% ($P = 0.0013$) (Table 4).

Effects of SAR340835 and Dobutamine on Left Ventricular Diastolic Function of Conscious HF Dogs. Infusion of SAR340835 did not significantly change the indices of diastolic function. LVEDP was reduced to a similar extent (−7.5%, −21.4%, and −16.3% after 250, 750, and 1500 μg/kg per hour, respectively), although these changes failed to reach the significance level as compared with vehicle-treated animals (Table 4).

Dobutamine infusion significantly improved dP/dt_{min} by 58.2% ($P = 0.0195$) and reduced LVEDP by 17.7% ($P = 0.0249$) but did not modify other parameters of diastolic function (Table 4).

Effects of SAR340835 and Dobutamine on Autonomic Nervous System in HF Dogs. SAR340835 significantly improved sympathovagal imbalance as evidenced by the significant decrease in the Low Frequency/High Frequency ratio observed at all doses ($P = 0.0112$, $P = 0.0008$, and $P = 0.0007$ at 250, 750, and 1500 μg/kg per hour, respectively)

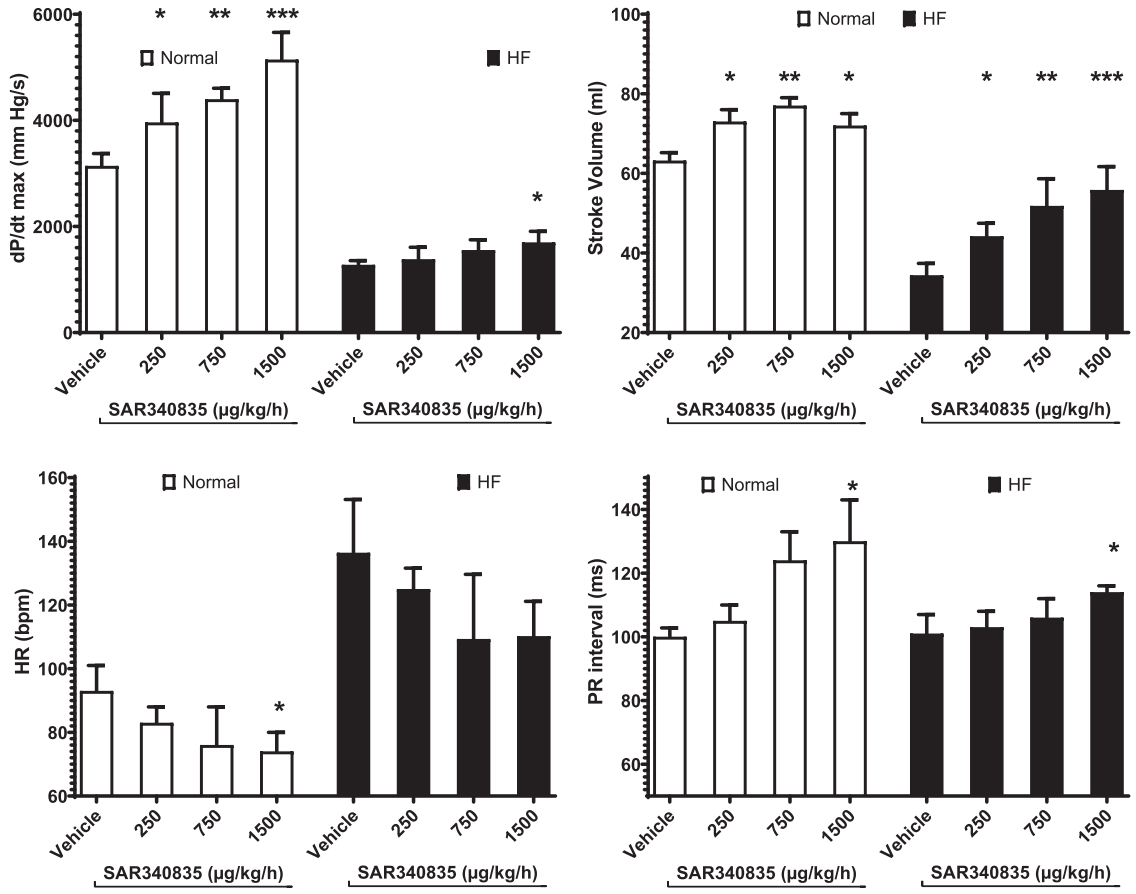

Fig. 4. Cardiac function in conscious normal and heart failure mongrel dogs. SAR340835 was administered as an intravenous bolus, followed by an intravenous infusion (see Table 1). Dose-dependent effects of SAR340835 on normal (□) and heart failure dogs (■) on dP/dt_{max}, SV, HR, and PR interval (n = 3–5 dogs). All data are expressed as means ± SEM $^*P < 0.05$, $^{**}P < 0.01$, $^{***}P < 0.001$ vs. vehicle for each condition.

(Fig. 5; Table 4). SAR340835 significantly improved baroreflex sensitivity (BRS) in a dose-dependent manner (+55.6%, P = 0.0304; +74.9%, P = 0.0048; and +119.6%, P = 0.0003, compared with vehicle, respectively) (Fig. 5; Table 4). Dobutamine infusion did not change sympathovagal imbalance or baroreflex sensitivity as compared with vehicle (Table 4).

Effects of SAR340835 and Dobutamine on ECG Parameters of HF Dogs. SAR340835 infusion significantly increased PR interval duration after dose 3 in HF dogs (Table 2). Dobutamine infusion shortened PR interval significantly in HF dogs (Table 4). PR interval was 90 ± 2 milliseconds versus 101 ± 5 milliseconds in the dobutamine versus vehicle group, respectively. No AVBs were observed under SAR340835 infusion in HF dogs.

Effects of SAR296968 on HF Dog Cardiomyocytes

Detailed results of dog cardiomyocyte studies are provided in the Supplemental Material.

Discussion

The current work aimed at establishing the potential therapeutic value of SAR340835, a novel NCX inhibitor, for the treatment of AHF. We first demonstrated that SAR340835 is a potent inhibitor of NCX across the different isoforms with no effects on Ca^{2+} or Na^+ channels and with a similar potency in reverse and forward mode. In vivo and in vitro studies showed that SAR340835 displayed antiarrhythmic effects, improved systolic function, reduced HR, and restored both sympathovagal balance and BRS in HF dogs, exerting a more pronounced beneficial cardiac effect in HF than in normal conditions without changing the calculated MVO2. Interestingly SAR340835 pharmacodynamic profile differed notably from dobutamine, the inotrope of reference for AHF.

NCX expression and activity are upregulated in human and animal failing heart (Hasenfuss et al., 1999; Sipido et al., 2002), thereby contributing to cardiac dysfunction in HF (Hobai et al., 2004) and EAD- and DAD-related arrhythmias typically occurring in patients with HF (Sipido et al., 2002). Consistently NCX inhibition displayed antiarrhythmic properties (Tanaka et al., 2007; Milberg et al., 2008). This was confirmed with SAR340835, which strongly inhibits the occurrence of ventricular and atrial arrhythmias in various experimental conditions, stimulating NCX inward current in guinea pig, rabbit, or pig. Thus, SAR340835 suppressed DAD-related arrhythmias at concentrations that increased cardiac contractility in guinea pig isolated papillary muscles and atria. SAR296968 efficiently reduced long QT–related arrhythmias at concentrations matching those that increased SV in HF dog. Overall, these results suggested a marked antiarrhythmic profile that is probably devoid of proarrhythmic property since no direct activity was detected on K^+, Na^+, or Ca^{2+} channels. Indeed, patch-clamp studies supported the

TABLE 3

Hemodynamics and LV function in conscious dogs before and after development of pacing-induced heart failure (n = 5 to 6)

Autonomic nervous system was evaluated by heart rate variability analysis. All data are expressed as means ± SEM and median ± MAD for Low Frequency/High Frequency ratio.

	Before Pacing Normal Dogs (n = 5 to 6)	After Pacing HF Dogs (n = 5 to 6)
Hemodynamics		
dP/dt_{max} (mm Hg/s)	3082 ± 300	1249 ± 55**
dP/dt_{min} (mm Hg/s)	−3104 ± 152	−1487 ± 112***
LVEDP (mm Hg)	11.0 ± 1.6	33.2 ± 3.7**
SBP (mm Hg)	122.3 ± 5.6	104.3 ± 4.7***
DBP (mm Hg)	92.0 ± 6.0	79.3 ± 5.5**
dP/dt_{max}/LVEDV (mm Hg/s per milliliter)	43.5 ± 5.6	10.8 ± 1.1**
MVO2 (ml O_2/min per 100 gram)	13.0 ± 1.27	13.3 ± 1.02
Echocardiography		
SV (ml)	64 ± 2	31 ± 3**
HR (bpm)	87 ± 6	149 ± 9**
CO (l/min)	5.2 ± 0.5	4.3 ± 0.4
LVEF (%)	55 ± 3	28 ± 1***
LVEDV (ml)	75 ± 6	119 ± 6**
E (cm/s)	0.85 ± 0.051	0.872 ± 0.029
DT (ms)	83.6 ± 7.1	54.3 ± 4.4**
A (cm/s)	0.608 ± 0.042	0.423 ± 0.027**
E/A	1.41 ± 0.07	2.08 ± 0.07***
Heart rate variability		
Low Frequency (nu)	19 ± 4	61 ± 3***
High Frequency (nu)	78 ± 5	27 ± 2***
Low Frequency/High Frequency	0.22 ± 0.12	2.29 ± 0.45***
BRS (mm Hg/s)	49 ± 3	24 ± 3**

High Frequency, parasympathetic modulation; Low Frequency, sympathetic modulation; Low Frequency/High Frequency; sympathovagal balance; nu, normalized unit.

*$P < 0.05$, **$P < 0.01$, and ***$P < 0.001$ HF vs. Normal condition.

high selectivity of SAR296968 for NCX versus these ion channels.

Beyond its antiarrhythmic effects, prolonged infusion of SAR340835 markedly improved the systolic cardiac function. Such an effect was expected with NCX inhibition (O'Rourke et al., 1999; Otsomaa et al., 2020) but was not yet demonstrated in vivo in conscious large-species models of HF. SAR340835 increased systolic function at similar exposure in normal and HF dogs but with different associated cardiodynamic changes. In normal dogs, SAR340835 significantly and dose-dependently increased cardiac contractility as evaluated by dP/dt_{max}, whereas the increase in SV plateaued from the first dose, probably because of the naturally high cardiac performance at baseline in normal conditions. Conversely, a marked and dose-dependent increase in SV revealed the improvement of systolic function in HF dogs more clearly than the increase in dP/dt_{max}. The dP/dt_{max} estimation of cardiac contractility depends on preload and afterload, and the large difference in cardiac load conditions at baseline between normal and HF dogs might have influenced the response on dP/dt_{max}. Overall, SAR340835 was more efficient in improving cardiac pump function in HF than in normal condition.

In isolated HF dog cardiomyocytes, SAR296968 at the highest concentration tested significantly increased sarcomere shortening and contraction velocities to the same extent as dobutamine. Interestingly, SAR296968 had no contractile effect in normal dog cardiomyocytes, whereas dobutamine increased sarcomere shortening to the same magnitude in both preparations. This larger effect of NCX inhibition agrees with the literature. Often, the inotropic effects reported with NCX inhibitor are weak or nil in normal canine cardiomyocytes (Birinyi et al., 2008; Oravecz et al., 2018). Interestingly, partial inhibition of NCX with the exchanger inhibitory peptide XIP improved the Ca^{2+} transient amplitude more in failing than in normal canine cardiomyocytes (Hobai et al., 2004). This was not unexpected considering the reported overexpression of NCX in human (Goldhaber and Philipson, 2013) and canine failing hearts (Winslow et al., 1999; O'Rourke et al., 1999), leading to premature Ca^{2+} efflux, reduced sarcoplasmic reticulum Ca^{2+} content, and impaired cell contractility. Then, partial inhibition of NCX could be enough to regulate disturbed calcium handling due to NCX overactivity and thus better improve the cardiac contractility than in normal condition.

On the other hand, other factors besides the augmented cardiac contractility could promote an increase in SV. In HF dogs, we observed that SAR340835 corrected the autonomic tone and BRS deficiency from the first dose tested while reducing the HR, in contrast with dobutamine. These beneficial effects of SAR340835 were comparable to those reported after chronic electrical stimulation of the carotid sinus baroreflex in HF dogs (Zhang et al., 2009; Sabbah et al., 2011). Indeed, ANS disturbances have been studied extensively in the HF condition (Shen et al., 2002; Zucker et al., 2007; Zhang et al., 2009). Overall, the autonomic balance shifts from primarily dominant vagal tone in the normal condition to sympathetic predominance in HF. The pathophysiological role of sympathetic activation in HF is highlighted by the beneficial effects of β-blocker therapy. The functional weakness of parasympathetic activity was observed in clinical and experimental HF (Floras and Ponikowski, 2015), from the early stages of HF (Ishise et al., 1998), and rising with disease progression (van Bilsen et al., 2017). Furthermore, the diminished cardiac vagal activity, increased HR, and decreased BRS are predictors of high mortality rate in patients with myocardial infarction or HF (La Rovere et al.,

TABLE 4

Cardiac and hemodynamic effects of SAR340835 and dobutamine in HF dogs

Autonomic nervous system was evaluated by heart rate variability analysis. All data are expressed as means ± SEM and median ± MAD for Low Frequency/High Frequency ratio ($P < 0.05$ vs. vehicle group; n = 3–5 dogs according to the group or parameter considered).

		HF Dogs				
		Vehicle Infusion	SAR340835 Infusion			Dobutamine
	n		250μg/kg per hour	750μg/kg per hour	1500 μg/kg per hour	10 μg/kg per minute
Hemodynamics						
dP/dt_{max} (mm Hg/s)	3 to 4	1276 ± 79	1382 ± 225	1554 ± 195	1699 ± 208*	2037 ± 9$^{\#}$
dP/dt_{min} (mm Hg/s)	3 to 4	−1550 ± 42	−1643 ± 128	−1720 ± 117	−1726 ± 65	−2452 ± 194$^{\#}$
LVEDP (mm Hg)	3 to 4	36.8 ± 2.8	34.0 ± 4.4	30.0 ± 3.5	30.8 ± 3.8	30.3 ± 2.3$^{\#}$
SBP (mm Hg)	5	109.0 ± 4.4	105.8 ± 5.9	102.4 ± 5.2	111.0 ± 5.3	106.0 ± 2.2
DBP (mm Hg)	4 to 5	84.6 ± 4.2	80.0 ± 4.8	77.5 ± 4.7	83.4 ± 4.6	73.6 ± 3.5
dP/dt_{max}/LVEDV (mm Hg/s per milliliter)	3 to 4	11.4 ± 0.7	12.2 ± 1.5	13.1 ± 1.2	14.4 ± 1.5**	18.8 ± 1$^{\#}$
MVO2 (mlO_2/min per 100 gram)	4 to 5	13.2 ± 1.06	13.51 ± 0.52	12.51 ± 0.99	14.01 ± 1.03	16.93 ± 1.19$^{\#\#}$
PR interval (ms)	4 to 5	101 ± 5	103 ± 5	106 ± 6	114 ± 2*	90 ± 2$^{\#}$
Echocardiography						
SV (ml)	4 to 5	34 ± 3	44 ± 3*	52 ± 7**	56 ± 6***	60 ± 5$^{\#}$
HR (bpm)	4 to 5	136 ± 17	125 ± 7	109 ± 20	110 ± 11	133 ± 5
CO (l/min)	4 to 5	4.6 ± 0.2	5.6 ± 0.2	5.3 ± 0.5	5.8 ± 0.6	8.0 ± 0.7$^{\#\#}$
LVEF (%)	4 to 5	29 ± 3	34 ± 3	40 ± 3 *	41 ± 2**	43 ± 3
LVEDV (ml)	4 to 5	111 ± 2	110 ± 4	116 ± 4	118 ± 2	109 ± 2
E (cm/s)	4 to 5	0.912 ± 0.027	0.958 ± 0.071	0.965 ± 0.108	1.012 ± 0.078	1.088 ± 0.083
DT (ms)	4 to 5	56.2 ± 7.1	56.2 ± 3.0	61.8 ± 5.1	65.6 ± 3.0	57.3 ± 6.6
A (cm/s)	4 to 5	0.446 ± 0.027	0.472 ± 0.035	0.465 ± 0.044	0.472 ± 0.061	0.485 ± 0.031
E/A	4 to 5	2.07 ± 0.11	2.05 ± 0.13	2.16 ± 0.38	2.22 ± 0.22	2.25 ± 0.15
Heart rate variability						
Low Frequency (nu)	4 to 5	55 ± 4	31 ± 4**	21 ± 2 ***	24 ± 5***	48 ± 3
High Frequency (nu)	4 to 5	35 ± 4	66 ± 4**	74 ± 4 ***	73 ± 5***	43 ± 6
Low Frequency/High Frequency	4 to 5	1.51 ± 0.40	0.44 ± 0.06*	0.28 ± 0.06 ***	0.31 ± 0.09***	0.95 ± 0.14
BRS (mm Hg/s)	4 to 5	32 ± 3	50 ± 4*	55 ± 4**	70 ± 4***	29 ± 2

High Frequency, parasympathetic modulation; Low Frequency, sympathetic modulation; Low Frequency/High Frequency, sympathovagal balance; nu, normalized unit.
*$P < 0.05$, **$P < 0.01$, and ***$P < 0.001$ SAR340835 vs. vehicle.
$^{\#}P < 0.05$, $^{\#\#}P < 0.01$, and $^{\#\#\#}P < 0.001$ dobutamine vs. vehicle.

1998; Lechat et al., 2001). Accordingly, several clinical studies have used stimulation devices, like vagal nerve stimulation or baroreceptor activation therapy, to reduce sympathetic nervous system reflex activity or promote vagal activity to restore a proper ANS balance (Singh et al., 2014). However, while the vagal nerve stimulation or baroreceptor activation therapy worked in animal models, clinical studies have been disappointing (van Bilsen et al., 2017).

The mechanisms provided by SAR340835 that lead to ANS balance restoration and the slight but consistent negative chronotropic effect are probably the end results of complex changes into electromechanical machinery underlying cardiac activity. Since HR was unaltered in NCX Knock Out mice or in mice overexpressing NCX, a direct role of NCX on pacemaker cells is unlikely (Gao et al., 2013; Kaese et al., 2017). However, NCX is an essential effector in β-adrenergic–mediated chronotropy (Gao et al., 2013; Kaese et al., 2017). Therefore, in HF conditions combining NCX and sympathetic overactivity, one might expect that NCX inhibition is likely to reduce HR, as observed in our HF dogs. However, we could not exclude that

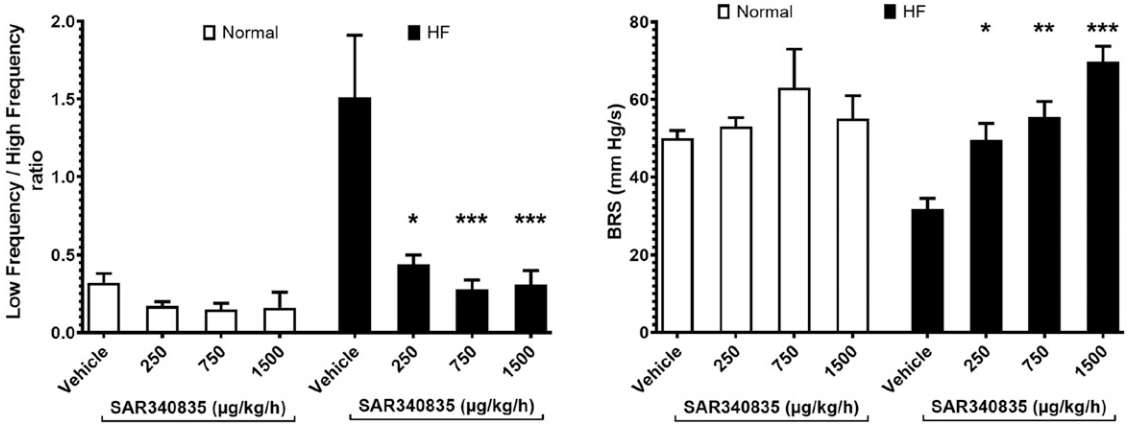

Fig. 5. Autonomic function in conscious normal and in heart failure mongrel dogs. SAR340835 was administered as an intravenous bolus, followed by an intravenous infusion (see Table 1). Dose-dependent effects of SAR340835 on normal (□) and heart failure dogs (■) on the Low Frequency/High Frequency ratio and BRS (n = 4 to 5 dogs). All data are expressed as means ± SEM for BRS and median ± MAD for the Low Frequency/High Frequency ratio. *$P < 0.05$, **$P < 0.01$, ***$P < 0.001$ vs. vehicle for each condition.

SAR340835-mediated bradycardia could be the consequence of restored sympathovagal balance and BRS, as previously reported for other positive inotropes that increased intracellular Ca^{2+} concentrations. Na^+ channel enhancer (Shen et al., 2002) and Ca^{2+} channel activator (Uechi et al., 1998) both reduced HR and enhanced BRS in pacing-induced HF dogs but not in normal dogs. Using ganglionic or β-adrenergic blockade, these authors demonstrated that the negative chronotropic effect was mainly due to an increased parasympathetic tone. The Ca^{2+} channel activator was hypothesized either to enhance BRS due to local alterations in the Na^+ content of the vessel wall (Kunze and Brown, 1978) or to exert a central neuronal mechanism increasing the vagal tone through intracellular Ca^{2+} elevation (Uechi et al., 1998). A close mode of action can reasonably be hypothesized for SAR340835, which similarly increased intracellular Ca^{2+} and showed the same pharmacological in vivo profile, but further studies are warranted to confirm this hypothesis. Additional beneficial effects of NCX inhibitors would be related to their antiarrhythmic properties, as they did not affect the refractory periods in ECG time intervals but slightly accelerated repolarization. This contrasts with Na+ channel enhancers, which prolong action potential duration and can promote EADs and torsade de pointes, and with Ca^{2+} channel activators also known to induce EADs and DADs (Chang et al., 2012; Shryock et al., 2013).

The attractiveness of NCX inhibition for the treatment of AHF could be compromised by the occurrence of second-degree AVB reported in normal dogs. However, SAR340835 at the highest dose tested showed only a limited prolongation effect on the PR interval in HF dogs and did not induce second-degree AVB. The high vagal tone characterizing normal dogs and the profound electrophysiological remodeling of failing hearts (including NCX overactivity) could partly explain these contrasting results between HF and normal conditions.

Overall, SAR340835 displays an attractive therapeutic profile for patients with HF, contrasting with current inotropes, reducing afterdepolarization-related arrhythmias, and improving systolic cardiac function without changing blood pressure or impairing the diastolic function. SAR340835 restored the impaired baroreflex sensitivity in HF dogs, thereby improving the balance between sympathetic and parasympathetic tone while maintaining potent β-adrenergic–independent inotropic effects. In addition, the slight bradycardia reported with SAR340835 could contribute to a reduction in myocardial oxygen consumption and improve cardiac efficiency, a valuable property in the setting of AHF. Accordingly, in HF dogs, the calculated MVO2 remained unchanged regardless of the dose of SAR340835, whereas it was raised with dobutamine infused in a therapeutic dose range. These promising results warrant further studies comparing SAR340835 and dobutamine at doses inducing a similar increase in cardiac contractility. Altogether, these results show that potent selective NCX inhibitors offer new therapeutic opportunities for the treatment of patients with AHF. Whether this efficacy would be observed in HF with preserved ejection fraction (HFpEF) as well as in HF with reduced ejection fraction conditions remains to be determined. Experimental studies (Kamimura et al., 2012; Primessnig et al., 2019) suggested that chronic partial NCX inhibition could be beneficial in HFpEF through normalization of overactivity of NCX. Moreover, several publications support the rationale for NCX overactivity in patients with HFpEF (Pieske et al., 2002; Ashrafi et al., 2017). Next steps with SAR340835 would be to explore the potential benefit against diastolic dysfunction in HFpEF models and to characterize the safety risk and determine the safety margin before considering any clinical development in AHF.

Acknowledgments

The authors of this manuscript would like to thank Dorothée Tamarelle for her statistical analysis and Maud Belot, Marie-Pierre Colas, and Olivier Blin for their excellent technical assistance.

Authorship Contributions

Participated in research design: Pelat, Barbe, Daveu, Guillon, Steinmeyer, Wirth, Gögelein, Arndt, Trellu, Lucats, Beauverger, Pruniaux-Harnist, Janiak, Chézaviel-Guilbert.

Conducted experiments: Pelat, Barbe, Daveu, Ly-Nguyen, Lartigue, Marque, Tavares, Ballet, Wirth, Gögelein, Arndt.

Contributed new reagents or analytic tools: Rackelmann, Weston, Bellevergue, McCort.

Performed data analysis: Pelat, Barbe, Daveu, Ly-Nguyen, Lartigue, Marque, Tavares, Ballet, Guillon, Steinmeyer, Wirth, Gögelein, Arndt.

Wrote or contributed to the writing of the manuscript: Pelat, Daveu, Guillon, Steinmeyer, Wirth, Janiak, Chézalviel-Guilbert.

References

Ashrafi R, Modi P, Oo AY, Pullan DM, Jian K, Zhang H, Gerges JY, Hart G, Boyett MR, Davis GK, et al. (2017) Arrhythmogenic gene remodelling in elderly patients with type 2 diabetes with aortic stenosis and normal left ventricular ejection fraction. *Exp Physiol* **102**:1424–1434.

Bär FW, Tzivoni D, Dirksen MT, Fernández-Ortiz A, Heyndrickx GR, Brachmann J, Reiber JHC, Avasthy N, Tatsuno J, Davies M, et al.; CASTEMI Study Group (2006) Results of the first clinical study of adjunctive CAldaret (MCC-135) in patients undergoing primary percutaneous coronary intervention for ST-Elevation Myocardial Infarction: the randomized multicentre CASTEMI study. *Eur Heart J* **27**: 2516–2523.

Bers DM, Despa S, and Bossuyt J (2006) Regulation of Ca2+ and Na+ in normal and failing cardiac myocytes. *Ann N Y Acad Sci* **1080**:165–177.

Birinyi P, Tóth A, Jóna I, Acsai K, Almássy J, Nagy N, Prorok J, Gherasim I, Papp Z, Hertelendi Z, et al. (2008) The Na+/Ca2+ exchange blocker SEA0400 fails to enhance cytosolic Ca2+ transient and contractility in canine ventricular cardiomyocytes. *Cardiovasc Res* **78**:476–484.

Bögeholz N, Schulte JS, Kaese S, Bauer BK, Pauls P, Dechering DG, Frommeyer G, Goldhaber JI, Kirchhefer U, Eckardt L, et al. (2017) The effects of SEA0400 on Ca^{2+} transient amplitude and proarrhythmia depend on the Na^+/Ca^{2+} exchanger expression level in murine models. *Front Pharmacol* **8**:649.

Chang MG, Chang CY, de Lange E, Xu L, O'Rourke B, Karagueuzian HS, Tung L, Marbán E, Garfinkel A, Weiss JN, et al. (2012) Dynamics of early afterdepolarization-mediated triggered activity in cardiac monolayers. *Biophys J* **102**:2706–2714.

Czechtizky W, Weston J, Rackelmann N, Podeschwa M, Arndt P, Wirth K, Goegelein H, Ritzeler O, Kraft V, Bellevergue P, and McCort G (2013) inventors, Sanofi SA, assignee. Substituted 2-(Chroman-6-Yloxy)-thiazoles and their use as pharmaceuticals. U.S. patent US8912224B2. 2013 Mar 21.

Floras JS and Ponikowski P (2015) The sympathetic/parasympathetic imbalance in heart failure with reduced ejection fraction. *Eur Heart J* **36**:1974–82b.

Gao Z, Rasmussen TP, Li Y, Kutschke W, Koval OM, Wu Y, Wu Y, Hall DD, Joiner ML, Wu XQ, et al. (2013) Genetic inhibition of Na+-Ca2+ exchanger current disables fight or flight sinoatrial node activity without affecting resting heart rate. *Circ Res* **112**:309–317.

Goldhaber JI and Philipson KD (2013) Cardiac sodium-calcium exchange and efficient excitation-contraction coupling: implications for heart disease. *Adv Exp Med Biol* **961**:355–364.

Gronda E, Seravalle G, Brambilla G, Costantino G, Casini A, Alsheraei A, Lovett EG, Mancia G, and Grassi G (2014) Chronic baroreflex activation effects on sympathetic nerve traffic, baroreflex function, and cardiac haemodynamics in heart failure: a proof-of-concept study. *Eur J Heart Fail* **16**:977–983.

Hasenfuss G, Schillinger W, Lehnart SE, Preuss M, Pieske B, Maier LS, Prestle J, Minami K, and Just H (1999) Relationship between Na+-Ca2+-exchanger protein levels and diastolic function of failing human myocardium. *Circulation* **99**:641–648.

Hobai IA, Maack C, and O'Rourke B (2004) Partial inhibition of sodium/calcium exchange restores cellular calcium handling in canine heart failure. *Circ Res* **95**: 292–299.

Ishise H, Asanoi H, Ishizaka S, Joho S, Kameyama T, Umeno K, and Inoue H (1998) Time course of sympathovagal imbalance and left ventricular dysfunction in conscious dogs with heart failure. *J Appl Physiol* **84** (4):1234–1241.

Kaese S, Bögeholz N, Pauls P, Dechering D, Olligs J, Kölker K, Badawi S, Frommeyer G, Pott C, and Eckardt L (2017) Increased sodium/calcium exchanger activity enhances beta-adrenergic-mediated increase in heart rate: whole-heart study in a homozygous sodium/calcium exchanger overexpressor mouse model. *Heart Rhythm* **14**:1247–1253.

Kamimura D, Ohtani T, Sakata Y, Mano T, Takeda Y, Tamaki S, Omori Y, Tsukamoto Y, Furutani K, Komiyama Y, et al. (2012) Ca2+ entry mode of Na+/Ca2+ exchanger as a new therapeutic target for heart failure with preserved ejection fraction. *Eur Heart J* **33**:1408–1416.

Kohajda Z, Farkas-Morvay N, Jost N, Nagy N, Geramipour A, Horváth A, Varga RS, Hornyik T, Corici C, Acsai K, et al. (2016) The effect of a novel highly selective inhibitor of the sodium/calcium exchanger (NCX) on cardiac arrhythmias in in vitro and in vivo experiments. *PLoS One* **11**:e0166041.

Kunze DL and Brown AM (1978) Sodium sensitivity of baroreceptors. Reflex effects on blood pressure and fluid volume in the cat. *Circ Res* **42**:714–720.

La Rovere MT, Bigger JT Jr, Marcus FI, Mortara A, and Schwartz PJ ATRAMI (Autonomic Tone and Reflexes After Myocardial Infarction) Investigators (1998) Baroreflex sensitivity and heart-rate variability in prediction of total cardiac mortality after myocardial infarction. *Lancet* **351**:478–484.

Lechat P, Hulot JS, Escolano S, Mallet A, Leizorovicz A, Werhlen-Grandjean M, Pochmalicki G, and Dargie H (2001) Heart rate and cardiac rhythm relationships with bisoprolol benefit in chronic heart failure in CIBIS II Trial. *Circulation* **103**: 1428–1433.

Menick DR, Renaud L, Buchholz A, Müller JG, Zhou H, Kappler CS, Kubalak SW, Conway SJ, and Xu L (2007) Regulation of Ncx1 gene expression in the normal and hypertrophic heart. *Ann N Y Acad Sci* **1099**:195–203.

Milberg P, Pott C, Fink M, Frommeyer G, Matsuda T, Baba A, Osada N, Breithardt G, Noble D, and Eckardt L (2008) Inhibition of the Na+/Ca2+ exchanger suppresses torsades de pointes in an intact heart model of long QT syndrome-2 and long QT syndrome-3. *Heart Rhythm* **5**:1444–1452.

O'Rourke B, Kass DA, Tomaselli GF, Kääb S, Tunin R, and Marbán E (1999) Mechanisms of altered excitation-contraction coupling in canine tachycardia-induced heart failure, I: experimental studies. *Circ Res* **84**:562–570.

Oravecz K, Kormos A, Gruber A, Márton Z, Kohajda Z, Mirzaei L, Jost N, Levijoki J, Pollesello P, Koskelainen T, et al. (2018) Inotropic effect of NCX inhibition depends on the relative activity of the reverse NCX assessed by a novel inhibitor ORM-10962 on canine ventricular myocytes. *Eur J Pharmacol* **818**:278–286.

Otsomaa L, Levijoki J, Wohlfahrt G, Chapman H, Koivisto A-P, Syrjänen K, Koskelainen T, Peltokorpi S-E, Finckenberg P, Heikkilä A, et al. (2020) Discovery and characterization of ORM-11372, a unique and positively inotropic sodium-calcium exchanger/inhibitor. *Br J Pharmacol* **177**: 5534–5554 DOI: 10.1111/bph.15257.

Ottolia M, Torres N, Bridge JHB, Philipson KD, and Goldhaber JI (2013) Na/Ca exchange and contraction of the heart. *J Mol Cell Cardiol* **61**:28–33.

Peana D and Domeier TL (2017) Cardiomyocyte Ca2+ homeostasis as a therapeutic target in heart failure with reduced and preserved ejection fraction. *Curr Opin Pharmacol* **33**: 17–26.

Pieske B, Maier LS, Piacentino V 3rd, Weisser J, Hasenfuss G, and Houser S (2002) Rate dependence of [Na+]i and contractility in nonfailing and failing human myocardium. *Circulation* **106**:447–453.

Pott C, Eckardt L, and Goldhaber JI (2011) Triple threat: the Na+/Ca2+ exchanger in the pathophysiology of cardiac arrhythmia, ischemia and heart failure. *Curr Drug Targets* **12**:737–747.

Primessnig U, Bracic T, Levijoki J, Otsomaa L, Pollesello P, Falcke M, Pieske B, and Heinzel FR (2019) Long-term effects of Na^{+}/Ca^{2+} exchanger inhibition with ORM-11035 improves cardiac function and remodelling without lowering blood pressure in a model of heart failure with preserved ejection fraction. *Eur J Heart Fail* **21**:1543–1552.

Rooke GA and Feigl EO (1982) Work as a correlate of canine left ventricular oxygen consumption, and the problem of catecholamine oxygen wasting. *Circ Res* **50**:273–286.

Sabbah HN, Gupta RC, Imai M, Irwin ED, Rastogi S, Rossing MA, and Kieval RS (2011) Chronic electrical stimulation of the carotid sinus baroreflex improves left ventricular function and promotes reversal of ventricular remodeling in dogs with advanced heart failure. *Circ Heart Fail* **4**:65–70.

Shen W, Gill RM, Jones BD, Zhang JP, Corbly AK, and Steinberg MI (2002) Combined inotropic and bradycardic effects of a sodium channel enhancer in conscious dogs with heart failure: a mechanism for improved myocardial efficiency compared with dobutamine. *J Pharmacol Exp Ther* **303**:673–680.

Shryock JC, Song Y, Rajamani S, Antzelevitch C, and Belardinelli L (2013) The arrhythmogenic consequences of increasing late INa in the cardiomyocyte. *Cardiovasc Res* **99**:600–611.

Singh JP, Kandala J, and Camm AJ (2014) Non-pharmacological modulation of the autonomic tone to treat heart failure. *Eur Heart J* **35**:77–85.

Sipido KR, Volders PGA, Vos MA, and Verdonck F (2002) Altered Na/Ca exchange activity in cardiac hypertrophy and heart failure: a new target for therapy? *Cardiovasc Res* **53**:782–805.

Tanaka H, Shimada H, Namekata I, Kawanishi T, Iida-Tanaka N, and Shigenobu K (2007) Involvement of the Na+/Ca2+ exchanger in ouabain-induced inotropy and arrhythmogenesis in guinea-pig myocardium as revealed by SEA0400. *J Pharmacol Sci* **103**:241–246.

Uechi M, Asai K, Sato N, and Vatner SF (1998) Voltage-dependent calcium channel promoter restores baroreflex sensitivity in conscious dogs with heart failure. *Circulation* **98**:1342–1347.

van Bilsen M, Patel HC, Bauersachs J, Böhm M, Borggrefe M, Brutsaert D, Coats AJS, de Boer RA, de Keulenaer GW, Filippatos GS, et al. (2017) The autonomic nervous system as a therapeutic target in heart failure: a scientific position statement from the Translational Research Committee of the Heart Failure Association of the European Society of Cardiology. *Eur J Heart Fail* **19**:1361–1378.

Verwaerde P, Sénard JM, Galinier M, Rougé P, Massabuau P, Galitzky J, Berlan M, Lafontan M, and Montastruc JL (1999) Changes in short-term variability of blood pressure and heart rate during the development of obesity-associated hypertension in high-fat fed dogs. *J Hypertens* **17**:1135–1143.

Wei SK, Ruknudin AM, Shou M, McCurley JM, Hanlon SU, Elgin E, Schulze DH, and Haigney MCP (2007) Muscarinic modulation of the sodium-calcium exchanger in heart failure. *Circulation* **115**:1225–1233.

Winslow RL, Rice J, Jafri S, Marbán E, and O'Rourke B (1999) Mechanisms of altered excitation-contraction coupling in canine tachycardia-induced heart failure, II: model studies. *Circ Res* **84**:571–586.

Wirth KJ, Brendel J, Steinmeyer K, Linz DK, Rütten H, and Gögelein H (2007) In vitro and in vivo effects of the atrial selective antiarrhythmic compound AVE1231. *J Cardiovasc Pharmacol* **49**:197–206.

Zhang Y, Popovic ZB, Bibevski S, Fakhry I, Sica DA, Van Wagoner DR, and Mazgalev TN (2009) Chronic vagus nerve stimulation improves autonomic control and attenuates systemic inflammation and heart failure progression in a canine high-rate pacing model. *Circ Heart Fail* **2**:692–699.

Zucker IH, Hackley JF, Cornish KG, Hiser BA, Anderson NR, Kieval R, Irwin ED, Serdar DJ, Peuler JD, and Rossing MA (2007) Chronic baroreceptor activation enhances survival in dogs with pacing-induced heart failure. *Hypertension* **50**:904–910.

Address correspondence to: Dr Frédérique Guilbert, Sanofi R&D, 1 av. Pierre Brossolette, 91380 Chilly-Mazarin, France. E-mail: frederique.guilbert@sanofi.com

Online supplement

SAR340835, a novel selective NCX inhibitor, improves cardiac function and restores sympathovagal balance in heart failure.

Michel Pelat[1], Fabrice Barbe[1], Cyril Daveu[1], Laetitia Ly-Nguyen[2], Thomas Lartigue[1] , Suzanne Marque[1], Georges Tavares[1], Véronique Ballet[2], Jean-Michel Guillon[2], Klaus Steinmeyer[3], Klaus Wirth[3], Heinz Gögelein[3], Petra Arndt[3], Nils Rackelmann[3], John Weston[3], Patrice Bellevergue[4], Gary McCort[5], Marc Trellu[2], Laurence Lucats[1], Philippe Beauverger[1], Marie-Pierre Pruniaux-Harnist[1], Philip Janiak[1], Frédérique Chézaviel-Guilbert[1]

1: Authors are members of Cardiovascular and Metabolism TSU, Sanofi R&D, 1 avenue Pierre Brossolette, 91385 Chilly Mazarin, 2: Preclinical Safety, Sanofi R&D 3 Digue d'Alfortville 94140 Alfortville, 3: Sanofi R&D, Industriepark Höchst 65926 Frankfurt, 4: Integrated Drug Discovery, Sanofi R&D, 1 avenue Pierre Brossolette, 91385 Chilly Mazarin, 5: Integrated Drug Discovery, Sanofi R&D, 13 quai Jules Guesde, 94403 Vitry sur Seine

Online supplement

MATERIALS AND METHODS

Ethical approvals

All the procedures described in the present study were performed in agreement with the European regulation (2010/63/UE) and under the approval and control of SANOFI's ethics committee. All procedures were performed in AAALAC-accredited facilities in full compliance with the standards for the care and use of laboratory animals and in accordance either with the French Ministry for Research or with the German animal protection law.

In vitro characterization of SAR296968, the active principle of SAR340835

Effects of SAR296968 on CHO cells expressing sodium-calcium exchanger isoforms (NCX1, NCX2 and NCX3)

In vitro potency on the NCX isoforms was assessed by a cell-based calcium mobilization assay on Chinese hamster ovary (CHO) cell lines expressing either NCX1, NCX2 or NCX3 with a fluorescent imaging plate reader (FLIPR). The recombinant CHO-K1 cell lines stably expressing, respectively, the human NCX1, NCX2 and NCX3 were delivered by Steinbeis-Transferzentrum für Angewandte Biologische Chemie, Mannheim. Five recombinant CHO-K1 cell lines stably expressing dog, guinea-pig, pig, rabbit or rat NCX1 were generated in-house. The cells were kept in continuous culture under standard conditions (37°C, air supplemented with 5% CO_2) in HAM'S-F12 medium plus glutamine supplemented with 10% fetal calf serum (FCS) and 450 µg/ml G418. Cells were passaged every 3-4 days after detachment using a Trypsin solution and reseeded at a concentration of 150.000 cells/ml.

The assay was based on the measurement of the intracellular Ca^{2+}-concentration using the Ca^{2+}-sensitive dye Fluo4-AM. The ionophore Gramicidin (G-5002, SIGMA) was added to the cells during the measurements in the FLIPR, which elevates the intracellular Na^{+}-concentration and in turn leads to an increase in NCX activity in the "reverse" transport mode (Na^{+} out, Ca^{2+} in) resulting in an intracellular Ca^{2+} accumulation and a proportional increase in Fluo4-AM fluorescence. The increase in fluorescence was measured in cells being pre-incubated or not with SAR296968.

Fluorescence kinetics reflected NCX activity. To calculate the potency of NCX inhibition, the kinetics of the Fluo4-AM fluorescence increase was measured under conditions with fully active NCX or without NCX activity. The normal assay buffer is used as "high control" (100% NCX activity) and the assay buffer with 10 µM of a potent internal NCX inhibitor A000135933 (Hug *et al.* 2009) was used as "low control" (0% NCX activity). The inhibition of NCX was calculated in reference to the controls (0% inhibition = "low control", 100% inhibition = "high control") with the following formula:

Inhibition (%) 100 x [1 - (sample – low control)/(high control – low control)]

Selectivity profile of SAR296968

An extended profiling of SAR296968 was carried out by Eurofins Cerep SA (Targets listed in supplementary Table 4) using receptor-binding, ion channel-binding and enzyme assays. The binding of SAR296968 on these targets was assessed either by enzyme immunoassays, fluorometric, photometric, HTRF or radiometric assays. Functional assays were performed for BZD (benzodiazepine), 5-HT2B (serotonin type 2b), PR (progesterone) receptors, NE (norepinephrine) transporter and DA (dopamine) transporter.

Patch-clamp studies in guinea-pig cardiomyocytes

Activity of SAR296968 on the endogenous NCX (Iti), calcium (ICa) and sodium (INa) currents were investigated in normal guinea pig cardiac myocytes.

Preparation of single cardiomyocytes.

Guinea-pigs of either sex (Dunkin-Hartley Pirbright White, Möllegaard, Denmark, weight approximately 400 g) were sacrificed by concussion and exsanguination. The heart was quickly removed and retrogradely perfused via the aorta at 37°C: first for 5 min with Tyrode solution (in mM): NaCl 143, KCl 5.4, $MgCl_2$ 0.5, NaH_2PO_4 0.25, HEPES 5 and glucose 10, pH adjusted to 7.2 with NaOH; then the perfusion was continued with the same Tyrode solution, which now contained 0.015 mM $CaCl_2$ and 0.03% collagenase (type CLS II, Biochrom KG, Berlin, Germany) until tissue softened (~5-7 min). Thereafter, the heart was washed with storage solution containing (in mM) L-glutamic acid 50, KCl 40, taurine 20, KH_2PO_4 20, $MgCl_2$ 1, glucose 10, HEPES 10, EGTA 2 (pH 7.2 with KOH). The ventricle was cut into small pieces and myocytes were dispersed by gentle shaking. Cells were then filtered through a nylon mesh. Thereafter cells were washed twice by sedimentation and kept at room temperature in the same storage solution as described above.

Whole-cell patch-clamp recordings of the NCX currents

The whole-cell patch clamp technique (Hamill OP *et al.* 1981) was employed to measure ion currents from single isolated cardiomyocytes. Whole-cell currents were recorded with an EPC-10 patch clamp amplifier (HEKA Elektronik, Lambrecht, Germany) and Pulse software (HEKA, Lambrecht, Germany). A small aliquot of cell-containing solution was placed in a perfusion chamber and after a brief period allowing cell adhesion to the bottom, the chamber was continuously perfused with bathing solution (in mM): NaCl 140, KCl 4.7, $CaCl_2$ 1.3, $MgCl_2$ 1.0, HEPES 10, Glucose 10, pH adjusted to 7.4 with NaOH. Patch pipettes were pulled from borosilicate glass capillaries (Hilgenberg, Malsfeld, Germany) using a DMZ-Universal puller (Zeitz-Instruments, Munich, Germany) and were heat polished. When filled with pipette solution, they had a resistance of 2-3 MΩ. Offset voltages generated when the pipette was inserted in NaCl solution (1-5 mV) were zeroed before formation of the seal. After formation of the whole-cell mode, the series resistance was compensated by 40-60% and the electrical capacitance caused by the cell membrane was compensated by the EPC-10 compensation network. The cell capacitance amounted to 120-180 pF and the series resistance was 5-10 MΩ. The cell potential was -70 to -80 mV. After formation of the whole-cell voltage-clamp configuration, myocytes were kept at the holding potential of -80 mV. All patch-clamp experiments were performed under continuous perfusion of the cells with solution heated to 36±1°C. The pipette solution had the following composition (in mM): CsOH 160, CsCl 20, NaOH 20, $CaCl_2$ 29, $MgCl_2$ 2, TEA-Cl 20, aspartic acid 42, EGTA 42, ATP-Mg-salt, 10, HEPES 10, pH= 7.2 with CsOH. After obtaining the whole-cell mode, the bath solution was exchanged for the NCX-solution (in mM): NaCl 140, $CaCl_2$ 2, $MgCl_2$ 2, CsCl 2, BaCl2 1, NaH_2PO_4 0.33, nisoldipine 0.002, ouabain 0.02, HEPES 10, pH = 7.4 with NaOH.

Voltage ramps were applied from -120 mV to 60 mV in 1 s with frequency of 0.1 Hz. When currents were stable in the NCX solution, $NiCl_2$ (5 µM) was added to the bathing solution, causing complete and reversible inhibition of the NCX current. After wash-out of $NiCl_2$ SAR296968 was added at 10 nM concentration and the current was recorded after 5 min. Then the SAR296968 concentration was increased stepwise and recording time at each concentration was 5 min. Finally, $NiCl_2$ was added and current was recorded after 2 min.

Whole-cell patch-clamp recordings of the calcium and sodium currents

Conditions of whole-cell patch-clamp recordings of the calcium and sodium currents were as described for recording of NCX currents with the following differences. After establishing the whole cell configuration, the series resistance was usually < 10 MΩ and was compensated for voltage error due to the series resistance of the patch pipette. Data was acquired at 6.67 kHz and filtered with 2.87 kHz. All experiments were performed at room temperature. The pipette solutions for recording of voltage dependent Ca^{2+} and Na+ currents were either (in mM): CsOH 130, NaCl 8, MgCl2x6H2O 1, EGTA 10, HEPES 10, pH = 7.3 with CsOH or methanesulfonic acid (osmolarity 285 mOsmol), or (in mM): CsOH 130, CsCl 8, MgCl2x6H2O 1, MgATP 4, EGTA 10, HEPES 10, pH = 7.3 with CsOH or methanesulfonic acid (osmolarity 285 mOsmol). The Na+ free bath solution was (in mM): NMDG 125, CsCl 5, MgCl2 x 6H2O 1, Glucose 11.5, HEPES 10, TEA 20, CaCl2 1.8, pH = 7.4 with HCl/CsOH. For recording of voltage dependent Na^+ currents the pipette solution was (in mM): CsOH 130, CsCl 8, MgCl2 x 6H2O 1, MgATP 4, EGTA 10, HEPES 10, pH = 7.3 with CsOH or methanesulfonic acid (osmolarity 285 mOsmol), and the bath solution was (in mM): NMDG 125, CsCl 5, MgCl2x6H2O 1, Glucose 11.5, HEPES 10, TEA 20, CaCl2 1.8, NaCl 20, NiCl 0.1, Nifedipine 0.01, pH = 7.4 with HCl/CsOH.

For recording of voltage dependent Ca^{2+} currents cells were held at 80 mV and currents were routinely measured every 3 s by applying 500 ms voltage pulses to +10 mV. Current amplitudes were determined as maximal inward currents at +10 mV immediately before compound application and at the end of the experiment (≥1 min in the presence of compound). For recording of voltage dependent Na^+ currents, cells were held at 80 mV and currents were routinely measured every 5 s by applying 30 ms voltage pulses to +30 mV. Current amplitudes were determined as maximal inward currents at +30 mV immediately before compound application and at the end of the experiment (≥1.5 min in the presence of compound).

The difference between the current before application of the compound (control) and the last application of $NiCl_2$ was considered to be 100 %. The percent inhibition of the current at each concentration was evaluated related to this 100% value. The arithmetical mean ± standard error of the mean (SEM) of the percent inhibition data was obtained from the different experiments at each SAR296968 concentration.

Effects of SAR296968 on atrial and ventricular arrhythmias

The anti-arrhythmic properties of the NCX inhibitor were assessed in a battery of *in vitro* and *in vivo* models, using the active principle, SAR296968.

Delayed afterdepolarization (DADs)-related arrhythmias

The efficacy against DADs-related arrhythmias was tested in both guinea pig papillary muscles and left atria under calcium overload condition. Both preparations were mounted in an organ bath heated at 37°C, with one side on a hook connected to a pressure transducer (ISOTEC, Hugo Sachs Elektronik – Havard Apparatus, March-Hugstetten, Germany), and the other side fastened

with a small metallic tube to which gently negative pressure was applied. Action potentials (APs) were recorded by means of a glass microelectrode, filled with 3 M KCl solution. The electrodes were fabricated from borosilicate glass (item number: 1B150F-4, World Precision Instruments, Sarasota, USA) by means of a microelectrode puller (DMZ-Universal Puller, Zeitz Instruments, Martinsried, Germany). The electrodes had an electrical resistance of 5 to 10 megaohms. The electrical signal was recorded with an amplifier (Model 309, Harvard Apparatus GmbH, March-Hugstetten, Germany) and stored in a computer system.
Guinea-pig papillary muscles developed spontaneous contractions (DADs) when exposed to high extracellular calcium concentration (5.5 mM $CaCl_2$) and zero extracellular potassium concentration combined to bursts of rapid electrical pacing (4 Hz). These spontaneous contractions were counted over 6 seconds after pacing cessation, repeated before and 30 minutes after applying the active principle SAR296968 (1 and 3 µM) or the vehicle (0.3% DMSO). Additionally, the protective effect of SAR296968 (3µM) against guinea pig left atria spontaneous arrhythmic contractions was investigated. The arrhythmic contractions were induced after applying SAR296968 (3µM) or the vehicle (0.3% DMSO in saline) by combining a rapid electrical pacing and treatment with isoprenaline (1µM) and were counted over 6 seconds after termination of a rapid electrical pacing. In both models, contractility (dP/dt_{max}), relaxation (dP/dt_{min}) and action potential duration (APD) were measured using the computer software (ISO-2, MFK, Niedernhausen, Germany) at baseline and under SAR296968 exposure. For measurement of contractile force, the optimal tension to the isolated muscles as preload for force development was determined for each preparation.

Early afterdepolarizations (EADs)-related arrhythmias in isolated rabbit heart
The efficacy of SAR296968 against EADs was tested in isolated rabbit heart perfused according to the Langendorff method. The sinus node was crushed allowing low pacing stimulation. The model recapitulated Long QT syndromes (LQT) induced during 2 successive runs by combining either an activator of the late Na^+ channel (veratridine 0.5 µM, LQT2 model) or a hERG blocker (sotalol 50 µM, LQT3 model) with a period of bradycardia (40 bpm) and low potassium conditions (K^+ 1.5 mmol/L instead of 4 mmol/L;). The second run was repeated under treatments with either 0.3 or 1 µM SAR296968 or the vehicle (0.25% DMSO). The number of heart preparations in which intermittent or continuous Torsades de Pointes (TdP) episodes were observed during the period of hypokalemia and bradycardia was evaluated for each tested treatment. ECG parameters, recorded from electrogram obtained in a derivation-II like electrodes positioning, were measured at 80 and 40 bpm of pacing before and after treatments; they included QRS, QT, Tp-Te, a marker of the transmural dispersion of ventricular repolarization, evaluated by the time difference (ms) between the peak (Tp) and end (Te) of T wave (Antzelevitch *et al.* 1999).

Left atria vulnerability in anesthetized pigs
The anti-arrhythmic property of SAR296968 was further investigated by measuring the left atria vulnerability (LAV) in pentobarbital-anesthetized pigs. The purpose of this investigation was to find out what the effect of NCX-inhibition is on atrial refractoriness and electrically induced atrial arrhythmias. Pigs were premedicated with 2 mL Rompun® 2% i.m. (xylazine HCl, 23.3 mg/mL) and 1mL of Zoletil100® (100 mg/mL; 50 mg/mL Tiletamine and 50 mg/mL Zolazepam) and anesthetized with an i.v.-bolus of 3 mL Narcoren® (pentobarbital, 160 mg/mL) followed by a continuous intravenous infusion of 12-17 mg/kg/h pentobarbital. Pigs were ventilated with

room air and oxygen by a respirator. Blood gas analysis (pO2; pCO2) was performed at regular time intervals to control the oxygen supply via the respirator in order to maintain pO2 >100 mm Hg and pCO2 < 35-40 mm Hg. A left thoracotomy was performed at the fifth intercostal space, the lung retracted, the pericardium incised and the heart suspended in a pericardial cradle. The atrial effective refractory period, determined by the S1-S2 method, and cardiac contractility (dP/dt_{max}) were monitored at baseline and under treatment with SAR296968 (1.5 mg/kg over 20 minutes) solved in a mixture of DMSO (1mL) and PEG400 (9 mL). LAV was determined as described previously (Wirth *et al.* 2007). Briefly the S1-S2 stimulation procedure induced short self-terminating episodes of atrial tachycardia (fibrillation or flutter). The number of atrial repetitive action potentials following the premature beat S2 had to exceed 4 for a full score (1). Three or 4 repetitive action potentials were counted as a half score (0.5). The procedure was applied while increasing the coupling S1-S2 interval by 5 ms and repeated at 3 basic cycle lengths (150, 200 and 250 bpm). A total of 45 S1-S2 stimulation procedures were repeated before and after infusion of SAR296968 in 8 pigs. A separate control group of 7 pigs was performed according to the same protocol with infusion of the vehicle.

Effect of SAR340835 on cardiac hemodynamics in normal and HF dogs

Animal and Surgical Procedure

Twelve adult mongrel dogs (body weight 27 to 31 kg) were implanted with telemetry devices (L21-F2, Datasciences International, US). Six of them were additionally equipped with a pacemaker (Adapta® model, Medtronic, MI, USA) with bipolar epicardial Pacing Lead (CapSure® Epi, Medtronic, MI, USA) for induction of heart failure by tachypacing.

Dogs were sedated with acepromazine (0.75 mg/kg, IM, Calmivet® 1%, Vetoquinol, Magny-Vernois, France), 20 minutes before the induction of anaesthesia with an intravenous bolus of thiopental (20 mg/kg, IV, Thiopental® Inresa, Bartenheim, France). Anaesthesia was maintained, after intubation, with isoflurane (Isoflo® 2%, Zoetis, Malakoff, France).

The telemetry implant was placed under aseptic conditions between 2 abdominal muscular layers on the flank. Catheters and electrocardiogram (ECG) leads were tunneled until the 6th intercostal space. After a thoracotomy (5th intercostal space), the left ventricular pressure (LVP) catheter was introduced into the left ventricle via the apex (for the measurement of left ventricular pressure) and the aortic pressure (AP) catheter into the thoracic descending aorta (for the measurement of the aortic pressure). The 2 ECG leads were sutured on the left ventricle, one on the apex and one near the left atria. A pacemaker was implanted in 6 mongrels for the induction of HF by rapid pacing. The epicardial pacing leads were sutured on the right ventricle and wires were externalized in the inter-scapular area and connected to the pacemaker placed between 2 muscular layers on the back through another surgical incision. The thoracic incision was closed in layers and pneumothorax was evacuated.

Analgesia was ensured with a combination of buprenorphine (0.01 mg/kg, IM Vétergésic®, CEVA, Libourne, France) before thoracotomy, repeated in the evening of the surgical intervention and twice a day for 3 days. Then, meloxicam was administered once a day for 3 days (meloxicam, 0.2 mg/kg, IM Metacam®, Boehringer Ingelheim, Reims, France). Prophylactic antibiotherapy was ensured for 10 days by a mixture of benzylpenicillin procaine and dihydrostreptomycin (15 mg and 30 mg, IM respectively, Intramicin®, CEVA, Libourne, France). Body temperature and weight were periodically checked. Dogs were allowed to recover after surgery for a minimum period of 12 days. For drug infusion, dogs were implanted under anesthesia with a vascular access port (VAP, with 7Fr PU Catheter 60 cm SWIRL-MID-PU-C70

(Instech Solomon, Plymouth Meeting, PA, USA, Phymep, Paris France), the catheter of which being inserted into the jugular vein. The VAP was positioned into the inter-scapulae region. Dogs received post-surgical analgesia and non-steroidal anti-inflammatory drug (meloxicam, 0.2 mg/kg, IM Metacam®, Boehringer Ingelheim, Reims, France. After each surgical procedure, animals were isolated for a recovery period of 3 to 5 days.

Rapid Right Ventricular pacing-induced HF

Heart failure was induced by chronic rapid right ventricle pacing at 240 beats/min for 4 weeks with the programmable pacemaker. Baseline echocardiogram (see below) and hemodynamic recordings were performed before and at the end of the 4-week pacing period to assess the development of heart failure.

Study Design in normal and pacing-induced HF dogs

The same study design was applied to normal and HF dogs. All the experiments were performed in conscious animals 4 weeks after the induction of HF by rapid pacing. Dogs were daily trained to remain quiet during the hemodynamic and echocardiography procedures before and after surgery. Before each echocardiography and telemetry monitoring session, pacing was turned off and maintained off during the whole recording period.

Each animal was subjected to 4 treatment sessions over the two following weeks with vehicle or SAR340835 infused at 250, 750 or 1500 µg/kg/h. Pacing-induced heart failure dogs received dobutamine infused at 10 µg/kg/min during an additional session for comparison purpose. SAR340835 was intravenously administered with a loading dose over 2 min (0.29 mg/kg, 0.86 mg/kg or 1.73 mg/kg for 250, 750 and 1500 µg/kg/h, respectively) followed by a IV infusion maintained for 3 hours in HF dogs and 6 hours in normal dogs (250, 750 or 1500 µg/kg/h, respectively). For simplification, doses are designated by the maintenance infusion rate in the Tables and Figures. A minimum washout period of 2 days in accordance with the short half-life of compounds was allowed between two sessions.

During each session, after a 15-minute stabilization period, telemetry signals were continuously recorded throughout the treatment infusion. Echocardiography was performed before starting the treatment infusion and over the last minutes of the 3- or 6-hour treatment infusion.

Echocardiography Measurements

Cardiac function was assessed by echocardiography using a Philips CX 50 (Philips, Amsterdam, Netherlands) with a 5-MHz phased-array transducer. Right parasternal short axis view was performed to acquire M-mode on which end-diastolic and end-systolic diameter were measured. Right parasternal long axis view was performed to record a 4-chamber view on which left ventricular end-diastolic and end-systolic contouring was performed. The two latter were used to calculate end-diastolic and end-systolic volumes with the Simpson method of disks. Fractional shortening (FS) was calculated as $100 \times (LVEDD - LVESD)/LVEDD$ and ejection fraction was calculated as $100\times (LVEDV-LVESV)/LVEDV$). Additional methodological details are provided online in Supplemental methods.

Telemetry recordings and analysis

Telemetry signals (LVP, AP, ECG) were continuously recorded throughout the experiment starting 15 minutes before and until the end of vehicle or treatment infusion at a sampling rate of 500 Hz. Measurements were averaged over at least 20 seconds-periods using HEM software

(Notocord System, Croissy, France). Several derived parameters were calculated: diastolic (DBP) and systolic (SBP) aortic blood pressure, left ventricular end-diastolic pressure (LVEDP), dP/dt_{max} and dP/dt_{min}.

Oxygen consumption (MVO2) was calculated based on echocardiographic and telemetry parameters according to the formula (*Rooke and Feigl 1982*) :

$$MV02 = 0.000408*(SBP \times HR) +0.000325*[(0.8\ SBP + 0.2\ DBP) \times HR \times SV]/BW+1.43$$

Evaluation of autonomic tone and baroreflex

The effects of SAR340835 on the autonomic nervous system (ANS) were explored. Spectral analysis of heart rate variability (HRV) was performed for the evaluation of autonomic tone in all telemetered dogs before and at the end of the 3 hours of dosing. This spectral analysis using a fast Fourier transform algorithm on sequences of 512 points (5 minutes) was performed with the HEM CsA10 software (Notocord Systems, Croissy, France).

Specific frequency bands of HRV permitted the simultaneous assessment of sympathetic (Low Frequency (LF)) and parasympathetic (High Frequency (HF)) modulation with LF/HF ratio illustrating the sympathovagal balance. Spectral powers were determined as the area under the curve calculated for the Very Low Frequency (VLF: 0.04 to 0.05 Hz), Low Frequency (LF: 0.05 to 0.15 Hz), and High Frequency (HF: 0.15 to 0.5 Hz) bands. The results are expressed in normalized units (nu) for spectral indices calculated as follows:

LF nu (%) = (LF / (LF + HF)) * 100

HF nu (%) = (HF / (LF + HF)) * 100.

To investigate the ability of heart rate changes to counteract arterial blood pressure variations, spontaneous baroreflex efficiency was evaluated using the sequence method (Gronda *et al.* 2014, Verwaerde *et al.* 1999). Briefly, sequences of at least 5 beats in which the systolic blood pressure and the RR interval changed in the same direction were identified as baroreflex sequences. A linear regression (r^2 =0,85) was applied to each sequence to calculate the value of the slope. For each evaluation time, the value of spontaneous baroreflex efficiency is the mean slope of all baroreflex sequences obtained on 512 consecutive values of systolic blood pressure and heart rate.

ECG analysis

The ECG signals of all animals were examined for any test article-related abnormality in waveform morphology. The PR interval was evaluated on each dosing day, at least at each selected time-point, over a 60 seconds-period. Examination of 2nd degree AVB was performed on the totality of the 24-hour recording of ECG.

Dog cardiomyocytes studies

Cell preparation

Four Pacing-induced Heart Failure Mongrels dogs (Marshall BioResourcesNorth Rose, New York, United States, 14-35 kg) or five Normal Beagles (14-16 kg) were used to isolate cardiomyocytes. The anesthesia was induced with nesdonal (Thiopental® Inresa, Bartenheim, France) and maintained after intubation with isoflurane (Isoflo® 2%, Zoetis, Malakoff, France). Before left lateral thoracotomy heparin injection (Choay, France: 300 UI/kg iv) was performed and the heart was perfused with ice-cold cardioplegic solution *(*Custodiol®). The inferior and superior vena cava, the pulmonary artery and the aorta were clamped, and a cannula was inserted

into the aorta to retro-infuse the ice-cold-cardioplegic solution (Custodiol®) to induce rapidly cardiac arrest. After excision, the heart was stored in Custodiol®.
Normal and HF dogs' cardiomyocytes were isolated by the Langendorff technique as previously published (Volders *et al.* 1999, Molina *et al.* 2014). Left anterior coronary artery was cannulated and the left ventricle was washed for 20 minutes with an isolation solution (35 mM NaCl, 4.75 mM KCl, 1.2 mM KH2PO4, 10 mM Dextrose (D-Glucose), 134 mM Saccharose, 16 mM Na2HPO4, 25 mM NaHCO3, 10 mM HEPES). The flow was set to 60 mL/min and left ventricle digested for 10 to 20 min with isolation solution complemented with 0.5% BSA (#0881066, MP Biomedicals) and 1mg/ml of collagenase A (#11088793001, Roche). The epicardial layer was removed and finely chopped in Wash Solution (130 mM NaCl, 4.8 mM KCl, 1.2 mM KH2PO4, 5 mM Dextrose (D-Glucose), 25 mM HEPES, 1% BSA (A7906, Sigma-Aldrich)). The supernatant was removed, and cells resuspended three more times with Wash solution: Calcium Medium mix at increasing [Ca2+] from 0.3 to 1.2 mM. Freshly isolated cells in Calcium Medium (MEM: M 4780; Sigma, St Louis, MO USA) containing 1.2 mM [Ca2+] supplemented with 2.5% foetal bovine serum (N4762; Sigma), 1% penicillin–streptomycin (15140-122, Gibco), 20 mM HEPES (pH 7.6), were plated on 35 mm, laminin-coated culture dishes (10 mg/mL) at a density of 20103 cells per dish. After 1 h the medium was replaced by 1 mL of FBS-free medium.

Sarcomere shortening in dog cardiomyocytes
Sarcomere dynamics were recorded from cardiomyocytes using video-based cell geometry (IonOptix systems, Dublin, Ireland). Laminin-coated coverslips containing adherent cardiomyocytes were washed with Tyrode Solution containing 121 mM NaCl, 5.4 mM KCL, 4.0 mM NaHCO3, 0.8 mM Na2HPO4, 1.8 mM MgCl2, 5 mM glucose, 10 mM HEPES, 5 mM Na pyruvate and 1.8 mM CaCl2 (pH 7.4). Each coverslip was placed in a perfusion chamber (FHD chamber, IonOptix) mounted on the stage of an inverted microscope (Motic AE30/31).
Each coverslip was exposed to only one concentration and only one cardiomyocyte was recorded per coverslip. Signals were continuously recorded for the duration of the experiment. The myocytes were field stimulated at 0.5 Hz with suprathreshold voltage with a bipolar pulse of 3 ms duration (Myopacer stimulator, Ionoptix) using a pair of platinum wires placed on opposite sides of the chamber. All measurements were performed at room temperature. After a 100 stabilization period in Tyrode Solution (vehicle), perfusion was switched to SAR296968, dobutamine or Vehicle for 6 min. Myocytes were continuously perfused with Tyrode solution containing either SAR296968 (0.3, 1, 3 or 10 µM), dobutamine (1µM) or vehicle (0.3% BSA and 0.1% DMSO in Tyrode solution) depending on the group.
Parameters of interest were captured at the end of stabilization period (baseline) and at the end of SAR296968, dobutamine or vehicle perfusion period. Ten peaks were averaged at each time-points and analyzed for sarcomere length with IonWizard 6.3 software (IonOptix). Parameters quantifying sarcomere dynamics were deduced from this analysis. Contraction velocity (µm/s) was calculated as the maximum rate of change in sarcomere length during the contraction phase. The peak height (µm), which represents the amplitude of the sarcomere shortening, was calculated by subtracting sarcomere length at minimum value (contracted state) to sarcomere length at maximum value (relaxed state). The peak height measured under exposure to SAR296968 was normalized to the measurement performed before SAR296968 infusion in the same cell as followed: $Ratio\ Peak\ Height = Peak\ Height_{SAR} / Peak\ Height_{baseline}$. Parameters of diastolic function were Relaxation Velocity (µm/s) which was calculated as the maximum rate of change in sarcomere length during the relaxation phase and the Time to 50% relaxation.

Effects of SAR296968 on dog cardiomyocytes

Averaged results (Table S4) obtained from 3-4 hearts from pacing-induced HF dogs indicate that the amplitudes and velocities of sarcomere shortening were significantly increased by SAR296968. The inotropic effect is further illustrated in a representative superimposed trace (Figure S1).

Sarcomere shortening ratio values showed a significant increase in the SAR296968-treated groups reaching 1.69 and 2.12-fold at 3 and 10 µM, respectively vs. the vehicle group. The significant positive inotropic effect observed with dobutamine, tested as a reference positive control, was in the same range (about 2-fold of vehicle effect). Concomitantly the contraction velocity was amplified but did not reach significance. SAR296968 induces a significant increase in relaxation velocity at 10µM like dobutamine but none of the drugs showed any effect on the Time to 50% relaxation (Table S4).

The positive inotropic effects obtained with SAR296968 in HF dog cardiomyocytes were not observed in cardiomyocytes isolated from normal dog (Table S5). In the latter study, sarcomere shortening was unchanged by SAR296968 but increased by dobutamine (about 3-fold of vehicle effect).

Figure S1. Evaluation of positive inotropic effect of SAR296968 on isolated canine ventricular cardiomyocytes under HF conditions. (A) Representative traces of Sarcomere Length (SL) shortening under basal conditions (red) and after exposure to 3 µM SAR296968 (blue). The cells were paced using field stimulation at 0.5 Hz. (B) Pooled data from 3-4 canine hearts showing contractile parameters following treatment with SAR296968, Dobutamine or Vehicle. For each graph, individual values, median and interquartile range are represented. p-value significant at 5% level (comparison versus Vehicle; *: Dunnett's test for SAR296968 / #: Student test for Dobutamine). Further statistical details are available in Table 4.

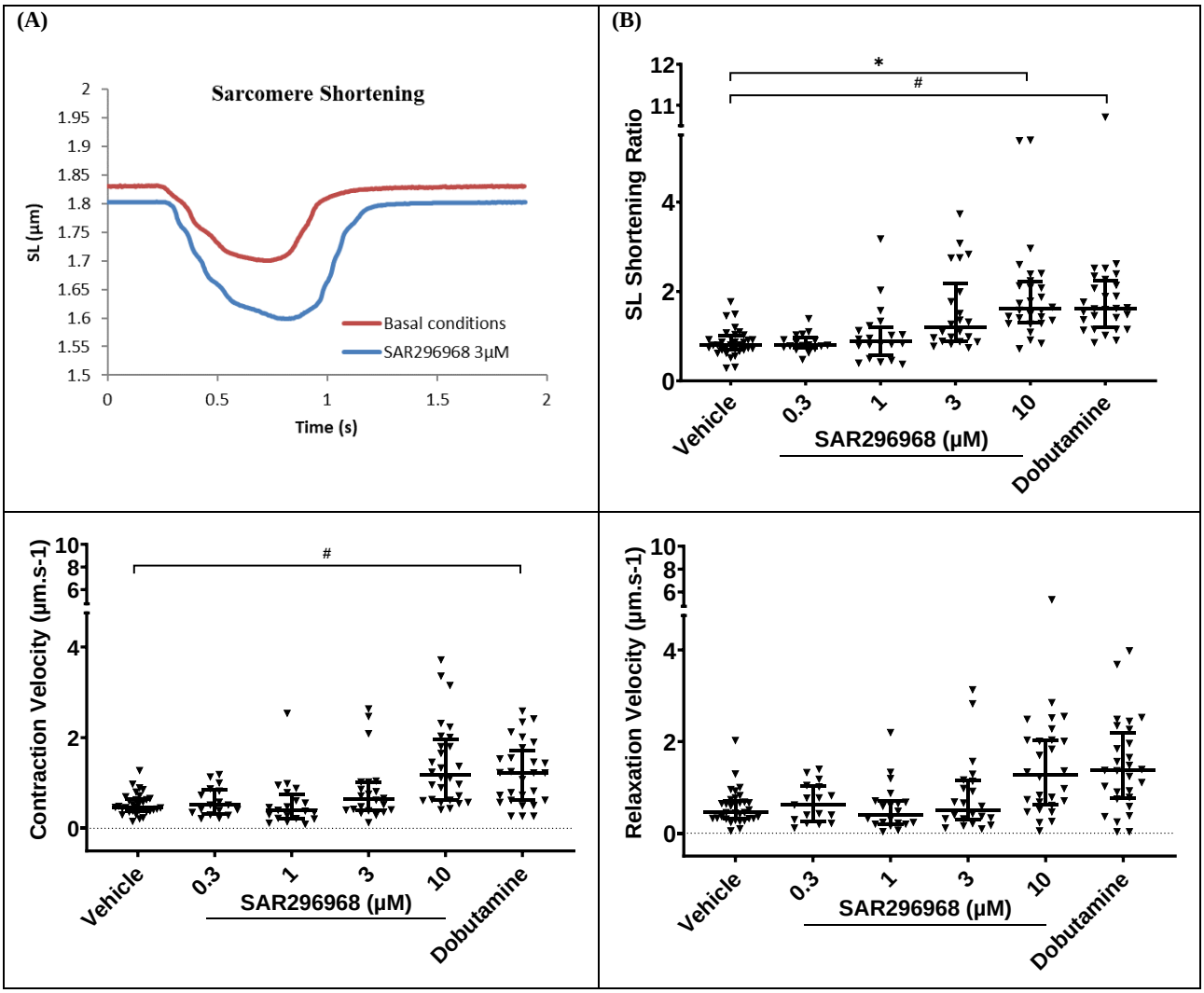

Table S1. Echocardiographic parameters were determined as described below:

Right parasternal short axis view was performed to acquire M-mode on which end-diastolic, end-systolic, fractional shortening and diameter aortic surface were measured			
Right parasternal short axis	Left Ventricular End Diastolic Diameter	LV EDD	mm
	Left Ventricular End Systolic Diameter	LV ESD	mm
	Left Ventricular Fractional Shortening[a]	LV FS	%
Right parasternal short axis	Aortic surface	Ao surf	cm^2
Right parasternal long axis view where end diastolic, end systolic volume were measured and Left ventricle ejection fraction was measured			
Right parasternal long axis view	Left Ventricular End Diastolic Volume	LV EDV	mL
	Left Ventricular End Systolic Volume	LV ESV	mL
	Left Ventricular Ejection Fraction[b]	LV EF	%
Left parasternal long axis view where Pulse wave Doppler was performed to measure Aortic and Mitral flow			
Pulse wave Doppler – aortic flow			
Left parasternal long axis view	Velocity time integral	VTI	cm
	Aortic Ejection Time	Ao ET	ms
Pulse wave Doppler – mitral flow			
Left parasternal long axis view	Peak velocity of early diastolic transmitral flow	E peak	cm/s
	Peak velocity of late transmitral flow	A peak	cm/s
	Deceleration time	DT	ms
	Duration of the A Wave	MV A duration	ms
	Ratio E/A	E/A ratio	-
Parameters calculated			
-	Stroke volume [c]	SV	mL
-	Cardiac output [d]	CO	L/min

a LV FS = [(EDD-ESD)/EDD]

b LV EF = [(EDV-ESV)/EDV]

c SV = [VTI * Ao surf]

d CO = [SV * HR] where HR is measured during the VTI measure.

Table S2. Effects of SAR296968 (1 and 3 µM) on contractility parameters and action potential duration in guinea pig papillary muscles (median +/- median absolute deviation)

	Guinea-pig papillary muscles		
	Vehicle	**SAR296968 1 µM**	**SAR296968 3 µM**
	mean ± sem	**mean ± sem**	**mean ± sem**
Maximal force of contraction (µN)	2443 ± 444	3779 ± 526	4419 ± 1029
dP/dt max (µN/ms)	38 ± 6	49 ± 6	56 ± 12
dP/dt min (µN/ms)	-32 ± 5	-43 ± 6	-46 ± 10
APD90 (ms)	185 ± 6	157 ± 15	163 ± 10

Table S3a. Effect of SAR296968 on the left ventricular repolarization and the QRS interval in isolated rabbit heart pretreated with sotalol or veratridine.

	Rate (bpm)	Vehicle (n=6)		SAR296968 0.3 µM (n=6)		SAR296968 1 µM (n=6)	
QRS (ms)							
Baseline	80	35 ± 2		37 ± 4		37 ± 1	
First run (Sotalol)	80	37 ± 2		36 ± 3		38 ± 1	
Second run (Sotalol + treatment)	80	38 ± 1		36 ± 2	*ns*	39 ± 2	*ns*
	40	37 ± 1		38 ± 3	*ns*	39 ± 1	*ns*
QT (ms)							
Baseline	80	201 ± 10		195 ± 8		191 ± 7	
First run (Sotalol)	80	258 ± 17		257 ± 25		238 ± 29	
Second run (Sotalol + treatment)	80	299 ± 30		253 ± 13	*	209 ± 7	*
	40	330 ± 30		214 ± 17	*	170 ± 6	*
Tp-Te (ms)							
Baseline	80	20 ± 2		20 ± 2		23 ± 2	
First run (Sotalol)	80	31 ± 3		29 ± 5		28 ± 4	
Second run (Sotalol + treatment)	80	38 ± 9		28 ± 4	*ns*	34 ± 4	*ns*
	40	58 ± 27		31 ± 6	*	38 ± 6	*ns*
QRS (ms)							
Baseline	80	39 ± 2		36 ± 1		39 ± 1	
First run (veratridine)	80	41 ± 1		36 ± 2		39 ± 1	
Second run (veratridine + treatment)	80	41 ± 3		36 ± 2	*ns*	40 ± 2	*ns*
	40	40 ± 3		37 ± 1	*ns*	40 ± 2	*ns*
QT (ms)							
Baseline	80	205 ± 3		194 ± 11		196 ± 8	
First run (veratridine)	80	395 ± 9		357 ± 21		390 ± 30	
Second run (veratridine + treatment)	80	397 ± 6		344 ± 15	*	356 ± 19	*
	40	486 ± 15		409 ± 12	*	418 ± 24	*ns*
Tp-Te (ms)							
Baseline	80	20 ± 1		20 ± 2		24 ± 4	
First run (veratridine)	80	56 ± 3		50 ± 10		45 ± 9	
Second run (veratridine + treatment)	80	53 ± 5		51 ± 6	*ns*	43 ± 9	*ns*
	40	51 ± 5		43 ± 2	*ns*	69 ± 8	*ns*

Table S3b. Effect of SAR296968 on left and right atria refractory periods in anesthetized pigs at pacing rate of either 150, 200 or 250 bpm.

	Left atrium AERP			Right atrium AERP		
BCL (bpm)	**150**	**200**	**250**	**150**	**200**	**250**
Baseline	113 ± 9	106 ± 8	100 ± 7	181 ± 9	162 ± 8	148 ± 9
Vehicle	110 ± 9	105 ± 7	101 ± 6	186 ± 12	170 ± 12	150 ± 10
Baseline	137 ± 4	128 ± 4	118 ± 3	190 ± 6	173 ± 8	161 ± 8
SAR296968	140 ± 7	125 ± 7	117 ± 6	188 ± 8	176 ± 8	160 ± 9

Table S4. Effect of SAR296968 on contraction and relaxation of failing cardiomyocytes isolated from pacing-induced HF dogs (median +/- median absolute deviation); dobutamine was tested as a positive control; p-value significant at 5% level (comparison versus Vehicle; *: Dunnett's test for SAR296968 / #: Student test for dobutamine).

Treatment	Vehicle	SAR296968 (µM)				dobutamine 1µM
		0.3	1	3	10	
N (Dog Heart)	4	3	4	4	4	4
n (cells)	33	17	20	22	28	28
sarcomere shortening (µm) before treatment	0.127 +/- 0.029	0.129 +/- 0.050	0.105 +/- 0.042	0.07 +/- 0.026	0.118 +/- 0.058	0.091 +/- 0.026
sarcomere shortening (µm) after 6 minutes of treatment's perfusion	0.102 +/- 0.027	0.103 +/- 0.053	0.093 +/- 0.038	0.095 +/- 0.030	0.188 +/- 0.066	0.169# +/- 0.067
sarcomere shortening ratio	0.803 +/- 0.122	0.798 +/- 0.098	0.888 +/- 0.294	1.190 +/- 0.316	1.617* +/- 0.404	1.618# +/- 0.464
contraction velocity (µm/s)	0.466 +/- 0.113	0.516 +/- 0.220	0.392 +/- 0.178	0.642 +/- 0.246	1.18 +/- 0.586	1.225# +/- 0.578
relaxation velocity (µm/s)	0.454 +/- 0.185	0.617 +/- 0.397	0.401 +/- 0.223	0.51 +/- 0.340	1.283 +/- 0.739	1.371 +/- 0.607
time to relax 50% (s)	0.305 (n=31) +/- 0.182	0.191 +/- 0.079	0.277 (n=18) +/- 0.102	0.235 (n=20) +/- 0.146	0.247 (n=24) +/- 0.139	0.222 +/- 0.118

Median +/- Median Absolute Deviation

Table S5. Effect of SAR296968 on contraction and relaxation of Normal cardiomyocytes from Beagles (median +/- median absolute deviation); dobutamine as positive control; p-value significant at 5% level (comparison versus Vehicle; *: Dunnett's test for SAR296968 / #: Student test for dobutamine). The protocol is the same as used for HF cardiomyocytes and it is described in Material and Methods.

Treatment	Vehicle	SAR296968 (μM)			dobutamine 1μM
		1	3	10	
N (Dog Heart)	5	4	5	5	5
n (cells)	16	12	16	18	12
sarcomere shortening (μm) before treatment	0.128 +/- 0.052	0.151 +/- 0.053	0.129 +/- 0.027	0.143 +/- 0.041	0.092 +/- 0.041
sarcomere shortening (μm) after 6 minutes of treatment's perfusion	0.142 +/- 0.052	0.132 +/- 0.060	0.143 +/- 0.028	0.141 +/- 0.040	0.250# +/- 0.039
sarcomere shortening ratio	0.843 +/- 0.258	0.917 +/- 0.259	0.894 +/- 0.373	1.075 +/- 0.265	2.249# +/- 0.674
contraction velocity (μm/s)	-0.699 +/- 0.414	-0.953 +/- 0.567	-1.032 +/- 0.476	-1.413 +/- 0.672	-3.004 +/- 1.164
relaxation velocity (μm/s)	0.782 +/- 0.544	1.069 +/- 0.730	0.896 +/- 0.646	1.260 +/- 0.736	2.995 +/- 0.560
time to relax 50% (s)	0.381 +/- 0.123	0.380 +/- 0.076	0.349 +/- 0.077	0.310 +/- 0.048	0.310 +/- 0.059

Median +/- Median Absolute Deviation

Table S6. CEREP selectivity profile (78 targets)

Non-peptide receptors	
A_3 *(h)*	5-HT_{1D}
BZD (central)	5-HT_{2B}*(h)*
BZD (peripheral)	5-HT_{2C} *(h)*
$GABA_A$	5-HT_3 *(h)*
$GABA_{B(1b)}$ *(h)*	5-HT_4e *(h)*
kainate	5-HT_6 *(h)*
H_3 *(h)*	5-HT_7 *(h)*
H_4 *(h)*	σ (non-selective)
P2X	σ_{1A}
P2Y	
Peptide receptors	
AT_1 *(h)*	MC_4 *(h)*
AT2 *(h)*	NK_1 *(h)*
BB (non-selective)	NK_2 *(h)*
B_1 *(h)*	NK_3 *(h)*
B_2 *(h)*	Y_1 *(h)*
CCK_1 (CCK_A) *(h)*	Y_2 *(h)*
CCK_2 (CCK_B) *(h)*	NTS_1 (NT_1) *(h)*
ET_A *(h)*	NMU2 *(h)*
GAL_1 *(h)*	δ_2 (DOP) *(h)*
GAL_2 *(h)*	κ (KOP)
CXCR2 (IL-8B) *(h)*	NOP (ORL1) *(h)*
CCR1 *(h)*	sst (non-selective)
TNF-α *(h)*	$VPAC_1$ (VIP_1) *(h)*
CCR2 *(h)*	V_1a *(h)*
MCH_1 *(h)*	V_{1b} *(h)*
MC_3 *(h)*	V_2 *(h)*
Nuclear receptors	
GR *(h)*	AR *(h)*
ERα *(h)*	TR (TH)
PR *(h)*	
Ion channels	
Ca_{2+} channel (L, verapamil site) (phenylalkylamine)	K_{ATP} channel
Ca_{2+} channel (N)	
Amine transporters	
GABA transporter	norepinephrine transporter (h)
5-HT transporter *(h)*	dopamine transporter (h)
Kinases	
CaMK2α *(h)*	IRK *(h)* (InsR)
Non-kinase enzymes	
COX_1 *(h)*	cathepsin L *(h)*
COX_2 *(h)*	MMP-1 *(h)*
12-lipoxygenase *(h)*	tryptase *(h)*
constitutive NOS *(h)* (endothelial)	phosphatase 1B *(h)* (PTP1B)
$PDE4D_2$ *(h)*	PLC
ACE *(h)*	MAO-B *(h)*
cathepsin D *(h)*	

For further details on assays see online information at www.eurofinsdiscoveryservices.com.

Specific Statistical Analysis

For Inhibition of NCX transport activity on CHO Cell-lines.

Single experiments for inhibition of NCX transport activity were carried out using 10 concentrations of the test compound in double determination. Half-maximal inhibitory concentrations (IC50) of the compounds for transport inhibition were calculated with internal software Biost@t SPEED V2.0 LTS using the 4-parameter logistic model according to Ratkowsky and Reedy (1986).

The adjustment was obtained by non-linear regression using the Levenberg-Marquardt algorithm in SAS v9.1.3.

For inhibition of NCX, ICa and INa currents.

The values for half-maximal inhibition (IC50) and the Hill coefficient were calculated by fitting the data points of the concentration/response curves to the logistic function. Results were obtained with internal software Biost@t-SPEED v1.3 using the 4-parameter logistic model according to Ratkowsky and Reedy (1986) with lower asymptote constrained at 0 and upper asymptote constrained at 100 (if not otherwise stated). The adjustment was obtained by non-linear regression using the Marquardt algorithm in SAS v8.2 software under UNIX. IC50 are given with their confidence interval.

For DADs-related arrhythmias models

All data are expressed as mean ± SEM or as median ± MAD. The Levene test was used to check heterogeneity of variances for both the guinea-pig papillary muscles and left atria studies. Due to heterogeneous variances in the guinea-pig papillary muscles study the Kruskal-Wallis test was applied on the parameter 'number of arrhythmic contractions' followed by Wilcoxon multiple comparisons test with Bonferroni Holm correction versus the vehicle control group. For the other parameters, maximal force of contraction, contractility, relaxation and action potential duration only descriptive statistics was provided. For the guinea-pig left atria study, a Wilcoxon test was applied on the parameter 'number of arrhythmic contractions' between SAR296968 3 µM and the vehicle control group. For the parameter contractility separate paired t-tests were applied on log-transformed dP/dt_{max} values between baseline and subsequent 3 µM SAR296968 or vehicle administration. The paired differences in means of the log-transformed dP/dt_{max} values were converted to mean ratios via the anti-log transformation. P-values < 0.05 were regarded as statistically significant.

For study on Left atrial vulnerability (LAV)

The one or two factor Levene test was used to check heterogeneity of variances. The paired t-test for SAR296968 treated animals versus baseline was used for the parameter left ventricular contractility. A two-way ANOVA with factor treatment and repeated measures for factor time (baseline and treated level) was applied on parameter LAV using heterogeneous variances for factor treatment followed by a Winer analysis for effect of factor time for each level of factor treatment. For parameter AERP a two-way ANOVA with repeated measures on factor time (baseline and treated level) and on factor BCL (basic cycle length) was applied separately for left and right atrium of the SAR296968 treated group and of the vehicle treated group correspondingly. P-values < 0.05 were regarded as statistically significant.

For in vivo experiments in normal and HF-dogs:

First, to analyze the induction of pathology, for each variable, a paired Student t-test was performed to compare parameters before and after induction of heart failure by 4 weeks of pacing.

To analyze the SAR340835 effect versus vehicle and the Dobutamine effect versus vehicle, for each variable and each objective, a one-way analysis of variance was performed on the raw data with group as fixed factor and animal as random factor.

In case of significance of the group factor, for the first objective a Dunnett's test was performed to compare each treated group to the vehicle group. For both objectives, the differences between the groups were estimated as well as their 95% CI (with Dunnett's adjustment for multiplicity for the first objective), they were expressed as a percentage of the corresponding vehicle mean for an easier interpretation, except for the LF/HF ratio parameter which was expressed as a ratio versus vehicle. The significance level was taken to 0.05. For the LF/HF ratio, the analyses were performed on log-transformed data due to heterogeneous variances.

The statistical analyses were performed using SAS® version 9.4 for Windows 7.

For Contractility evaluation on Dogs Cardiomyocytes

The statistical analyses for the in vitro part were performed to evaluate the SAR296968 and then the dobutamine (positive reference) treatment effect.

For each objective, for normal Beagles dogs a mixed model with fixed factor group and random factors animal and animal*group was performed. For HF Mongrel dogs, a mixed model with fixed factors group, system and their interaction and random factors animal and animal*group was performed was performed; then a backward elimination was applied to simplify the model. The variances heterogeneity on group factor was considered depending on the parameter. Appropriate post-hoc analysis was performed. A rank or log-transformation was applied when appropriate.

Descriptive statistics were calculated on cells. The significance level is taken to 5%, except for the interaction test for which the significance level is taken to 10%.

The statistical analyses were performed using SAS® version 9.4 for Windows 7.

Online supplement References

Antzelevitch, C., Yan, G. -X., and Shimizu, W. (1999) Transmural dispersion of repolarization and arrhythmogenicity. Journal of Electrocardiology, 32 (supplement 1): 158−165.

Hamill, O. P., A. Marty, E. Neher, B. Sakmann, and F. J. Sigworth. (1981) Improved Patch-Clamp Techniques for High-Resolution Current Recording from Cells and Cell-Free Membrane Patches. Pflugers Archiv: European Journal of Physiology 391 (2): 85–100.

Hug M., Licher T., Geibel S. and Vollert H. “Fluorescence based assay to detect sodium/calcium exchanger "forward mode" modulating compounds.” WO/2009/115239, Published September 24, 2009.

Molina, Cristina E., Daniel M. Johnson, Hind Mehel, Roel L. H. M. G. Spätjens, Delphine Mika, Vincent Algalarrondo, Zeineb Haj Slimane, et al. (2014) Interventricular Differences in β-Adrenergic Responses in the Canine Heart: Role of Phosphodiesterases. Journal of the American Heart Association 3 (3): e000858. doi:10.1161/JAHA.114.000858.

Ratkowsky DA, Reedy TJ (1986) Choosing near-linear parameters in the four-parameter logistic model for radioligand and related assays. Biometrics 42:575-82.

Volders Paul G. A., Sipido Karin R., Carmeliet Edward, Spätjens Roel L. H. M. G., Wellens Hein J. J., and Vos Marc A. (1999) Repolarizing K+ Currents ITO1 and IKs Are Larger in Right Than Left Canine Ventricular Midmyocardium. Circulation 99 (2): 206–10.